A CFD STUDY ON COMPARISON OF HEAT TRANSFER PERFORMANCE OF WATER BASED GRAPHENE NANOPLATELETS NANOFLUIDS AND MULTIWALLED CARBON NANOTUBES NANOFLUIDS IN A CONCENTRIC TUBE HEAT EXCHANGER

2022

الجامعـــة الإسلاميـــة للتكنولوجيا
UNIVERSITE ISLAMIQUE DE TECHNOLOGIE
ISLAMIC UNIVERSITY OF TECHNOLOGY
DHAKA, BANGLADESH
ORGANISATION OF ISLAMIC COOPERATION

A CFD STUDY ON COMPARISON OF HEAT TRANSFER PERFORMANCE OF WATER BASED GRAPHENE NANOPLATELETS NANOFLUIDS AND MULTIWALLED CARBON NANOTUBES NANOFLUIDS IN A CONCENTRIC TUBE HEAT EXCHANGER

A Thesis by

MD Zahinul Hoq (170011039)
MD Jabir Rahim (170011008)

Department of Mechanical and Production Engineering

Islamic University of Technology

May (2022)

A CFD STUDY ON COMPARISON OF HEAT TRANSFER PERFORMANCE OF WATER BASED GRAPHENE NANOPLATELETS NANOFLUIDS AND MULTIWALLED CARBON NANOTUBES NANOFLUIDS IN A CONCENTRIC TUBE HEAT EXCHANGER

MD Zahinul Hoq, 170011039, Session: 2020-21

MD Jabir Rahim, 170011008, Session: 2020-21

Submitted in Partial Fulfillment

of the Requirements

for the Degree of

Bachelor of Science in Mechanical Engineering

DEPARTMENT OF MECHANICAL AND PRODUCTION ENGINEERING

May (2022)

CERTIFICATE OF RESEARCH

This thesis titled "A CFD Study on Comparison of Heat Transfer Performance of Water Based Graphene Nanoplatelets Nanofluids and Multiwalled Carbon Nanotubes Nanofluids in a Concentric Tube Heat Exchanger" submitted by MD Zahinul Hoq (170011039), MD Jabir Rahim (170011008) has been accepted as satisfactory in partial fulfillment of the requirement for the Degree of Bachelor of Science in Mechanical Engineering.

Supervisor

Dr. Arafat Ahmed Bhuiyan

Associate Professor

Head of the Department

Prof. Dr. Md. Anayet Ullah Patwari

Professor

Department of Mechanical and Production Engineering (MPE)

Islamic University of Technology (IUT)

DECLARATION

I hereby declare that this thesis entitled "A CFD Study on Comparison of Heat Transfer Performance of Water Based Graphene Nanoplatelets Nanofluids and Multiwalled Carbon Nanotubes Nanofluids in a Concentric Tube Heat Exchanger" is an authentic report of study carried out as requirement for the award of degree B.Sc. (Mechanical Engineering) at Islamic University of Technology, Gazipur, Dhaka, under the supervision of Arafat Ahmed Bhuiyan, PdD, Associate Professor, MPE, IUT in the year 2020-2021

The matter embodied in this thesis has not been submitted in part or full to any other institute for award of any degree.

MD Zahinul Hoq

Student ID: 170011039

MD Jabir Rahim

Student ID: 170011008

ACKNOWLEDGEMENT

We would like to express our gratitude to Dr. Arafat Ahmed Bhuiyan, our supervisor, whose knowledge and assistance were vital to us. We were able to overcome several challenges in our thesis thanks to his patient guidance throughout our final year. We'd like to express our gratitude to Dr. Md. Rezwanul Karim and Mr. Md. Jahid Hasan for their invaluable assistance. Their insightful comments inspired us to think more clearly and improve the quality of our work. Finally, we'd want to express our gratitude to our family and friends for their unwavering support during our journey.

Abstract

For the next generation of nanofluids, carbon nanomaterials are of tremendous interest. CnT and GnP, in particular, are extremely thermally conductive, and their usage in heat transfer nanofluids is a significant field of study. Using a concentric tube annular heat exchanger in the same operating circumstances, the heat transfer performance of GnP-nanofluid and MWCNT-nanofluid was investigated in this study. In the inner tube, the manufactured nanofluid flowed as a hot fluid in the reverse direction of a colder water flow in the annulus tube. The flow rate (1.5 L/min – 2.5 L/min) and concentration (0.01% – 0.35%) of nanofluid were varied in the experiment. At the same flow rates and nanofluid concentrations, the heat transfer coefficient of GnP-nanofluid was found to be greater than that of MWCNT-nanofluid. When an appropriate volumetric concentration is attained in both nanofluids, the favorable influence on heat transfer performance increase is at its peak. In comparison to MWCNT, our research reveals that GnP can increase heat transfer coefficient at lower volumetric concentrations and flow rates.

Table of Contents

List of Figures

List of Table

Nomenclature

L = length of leg of U-shape HX

t = thickness

d = diameter

u = velocity component in x-direction

v = velocity component in y-direction

w = velocity component in z-direction

k = thermal conductivity

T = temperature

t = time

p = pressure

ρ = density

Φ = Dissipation Function (describes the effect of viscous stress)

Subscript

o = outer

i = inner

e = effective

Acronym

HTC = Heat Transfer Coefficient

GnP = Graphene nanoparticle

CnT = Carbon nanotube

MWCnT = Multiwalled Carbon nanotube

Chapter - 1: Introduction

1.1 Nanofluids

A nanofluid is a suspension of nanoparticles (at least one dimension of which is below 100 nm) in a base-fluid, such as water, alcohol, oil, or refrigerant, among other examples. Over the course of the last three decades, nanofluid has received a great deal of interest in the fields of nanotechnology, thermal engineering, and a variety of other applications. Several studies have reported finding quantitative evidence of an increase in the thermal conductivity of distinct nanofluids as well as an improvement in the heat transfer capability of such nanofluids [1], [2]. The low thermal conductivity of conventional fluids like water, oil, and ethylene glycol is a primary limitation in the development of energy-efficient heat transfer medium. It is generally accepted that the primary factor influencing the heat transfer efficiency of thermal convection is the thermal conductivity of heat transfer fluids. It has been shown that suspending microscopic solid particles in fluids in order to affect the transport properties, flow characteristics, and heat transfer characteristics of the liquids is an efficient method for increasing the thermal conductivity of the fluids [3]. In comparison to the base fluid, the thermal characteristics of the carbon-based nanofluids exhibit a substantial improvement. However, due to its high price, its application in commercial settings is restricted. The vast majority of studies that have been written regarding carbon-based nanofluids (such as graphene, graphene oxide, carbon nanotubes, etc.) have mostly focused on the material's thermal conductivity [4], electrical conductivity [5], and applications [6]. Only a few carefully chosen papers have explored the many elements of its stability in various base fluids (water, ethylene glycol, propyl glycol, liquid paraffin, oil etc.). Xie et al. [5] found that the CNT-decane nanofluid was stable for a period of 1440 hours when the stabilizer oleylamine was used. When compared to the base cutting fluid, a higher nanoparticle concentration results in increased conductivity, viscosity, and density, as well as enhanced heat extraction. The ball-bearing effect, tribofilm polishing, sliding and rolling effects, and rolling and sliding effects are the primary contributors to the mechanism of heat extraction and friction reduction. In a similar vein, carried out a variety of studies on titanium (grade-2) alloy by employing

nanofluids composed of graphite, aluminum oxide, and molybdenum disulfide. According to the findings, the nanofluids based on graphite have the potential to significantly improve the machining properties. In a study somewhat similar to this one, investigated the effectiveness of graphite-based cutting fluids in the turning of medium steel manufactured of AISI 1045. According to the findings, graphite that was produced using cutting fluids as a foundation is a viable option that can help enhance machining performance.

1.2 Problem Statement

Research work on carbon-based nanofluids is much less compared to metal-oxide nanofluids. In this work a numerical validation has been done of an experimental paper which determined and compared the HTC of GnP and MWCnT nanofluids. The experiment was done for nanofluids of different nanoparticle concentration with different flow rates.

The HTC of GnP nanofluid and MWCnT nanofluid were determined and compared. The nanofluids were prepared for five different volume concentrations, i.e., 0.01%, 0.05%, 0.15%, 0.25% and 0.35%. For each set of nanofluids three different flowrates were used, i.e., 1.5L/min, 2L/min, 2.5L/min. Total thirty cases were analysed and their HTCs were compared.

The heat exchanger used in the experiment was a U-shaped tube in tube heat exchanger. The outer tube is annulus though which the inner tube is passed. The diameter of the inner tube is 9.5mm which has a thickness of 0.6mm. The diameter of the outer tube is 12mm with a thickness of 0.3mm. As illustrated in Figure *3* at the U bent the inner tube moves out form the outer tube hence, the U bent portion of the tubes aren't thermally contacted.

1.3 Goals and Objectives

Currently a significant amount of work has been being done on metal-oxide nanofluids. Carbon compound based nanofluids are new, and form the few experimental works they are been proven an efficient option as a nanofluid. From Figure 1 it can be noted that the maximum number of research works has been done on Alumina nanofluids, which is 1290. Research work on CNT nanofluids is very less.

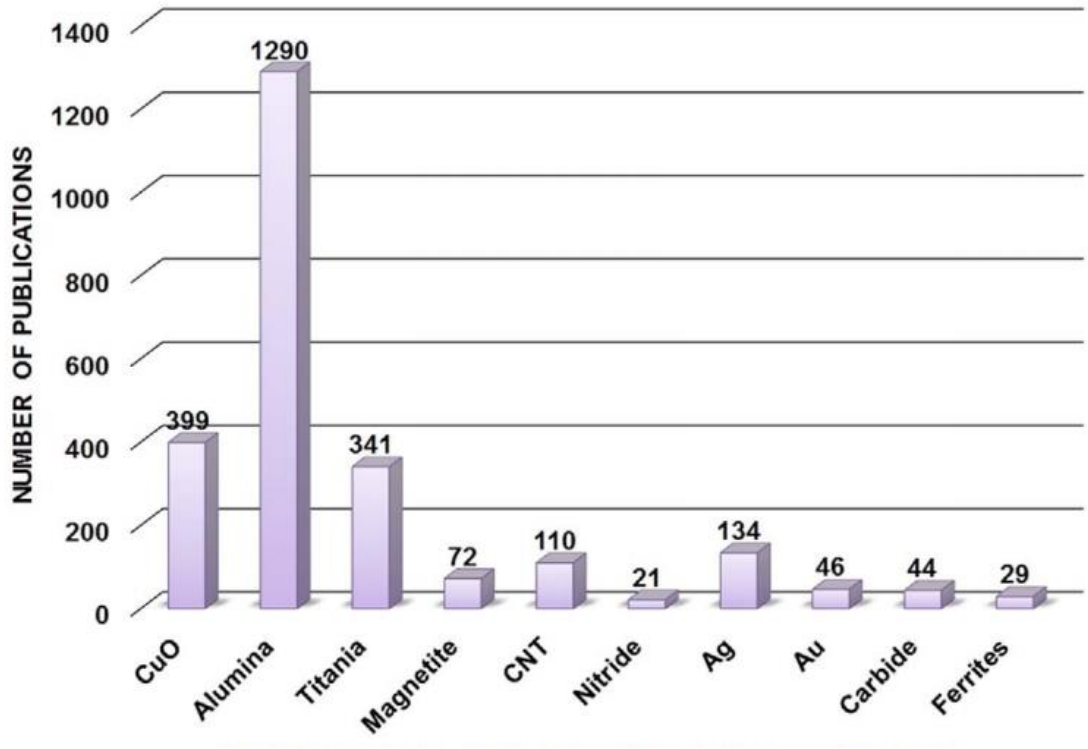

Figure 1: Nanomaterial category-wise distribution of nanofluids-related publications

The objective of this research is to perform a validation by numerical approach on an experimental work which compares the HTC between GnP nanofluids and MWCnT nanofluids both of which are carbon-based nanoparticles nanofluids.

The goal of this research is to compare the performance of carbon-based nanoparticles with metal oxide nanoparticles in their heat transfer capabilities.

Chapter - 2: Literature Review

Several studies have been done on the relation between HTC and weight concentration of nanoparticles. Also, relations are shown between HTC and Reynold's number. As Reynold's number and weight concentration of nanoparticles increases the flow approaches to turbulent regime. With increasing weight concentration and Reynold's number the HTC increases [7]. Along with increasing Reynold's number and weight concentration the rise of temperature difference and flow rate also results in the rise of HTC. A rise of 10K temperature difference can result in 10.7% increase in HTC [8]. Experiments conducted on GnP nanofluids of different weight concentration of 0.025%, 0.075% and 0.1% shows that with the increase in value of volumetric flow rate, the HTC also rises. And significant rise in HTC is observed with increase in weight concentration of the nanofluid irrespective of the flow sections [9]. The HTC of the nanofluid is highly dependent on the nano particle's thermo-physical properties, its Brownian velocity and the specific surface area. With the increase of specific surface area and Brownian velocity of the nano particles, the HTC rises steeply [10]. It is apparent that as the temperature and concentration rise, so does the local HTC. HTCs will improve as graphene concentration increases. It can be shown that when the temperature rises, the augmentation of the HTC increases. The increase in Brownian motion of particles with rising temperature could explain the improvement in thermal conductivity [11]. With the rise of nanofluid inlet temperature, the value of overall HTC drops. But by adding nanoparticles to the base fluid and rising the volumetric flow rate of the nanofluid improves the HTC significantly [12]. Experimental data using the Dittus-Boelter equation showed that the convection HTC increases with Reynolds number and volume concentration [13]. According to the findings of this investigation, using CuO and TiO2 nanoparticles as the dispersion in water can greatly improve convective heat transfer in the laminar flow regime, with the enhancement increasing with Dean number and particle concentration level under the conditions of this study [14]. The results reveal that dispersed nanoparticles significantly improve the base fluid's heat transfer performance, and the nanofluid has a higher HTC than pure water at the same Reynolds number. A nanofluid's heat transmission property improves as the volume fraction of nanoparticles grows [15]. From the experimental data, the TiO2-water nanofluid provides significant improvement of HTC than those of pure water at

the same Reynolds number. The convective HTC rises as the Reynolds number and mass flow rate of the heating fluid increase, and decreases as the nanofluid temperature decreases [16]. A nanofluid with lower particle size provides greater heat transmission for nanofluids of the same family (i.e. the same kinds of constituents) under the same flow rate and Reynolds number [17]. The addition of a modest amount of nanoparticle (0.0625 percent) to the base liquid significantly increased the HTC. Furthermore, increasing the Reynolds number increased the HTC. Furthermore, raising the volume concentration of nanoparticles can result in increased thermal conductivity, motivating one to raise the HTC of nanofluid [18]. Carbon nanotubes added to the base fluid can provide significant improvement of HTC and system's thermal behavior [19]. At the same Peclet number, adding nanoparticles to the base fluid improves heat transfer performance and resulting in a higher HTC than the base fluid [20]. With the increase of Reynolds number and volume fraction of the nanofluid, the local HTC also increases [21]. The local and average HTCs at a particular Reynolds number rises as the concentration of nanoparticles increases. At a constant flow rate, a decrease in HTC with higher particle concentration is possible. At a constant flow rate, the HTC of the nanofluid in the turbulent regime increases with increasing nanoparticle size [22]. With higher nanoparticle concentration and smaller copper tube diameter, the HTC of nanofluid is significantly raised [23]. The local convective HTC increases with increasing carbon nanotube concentration, and CNT nanofluid samples have a significantly higher HTC than distilled water [24]. The HTC of the nanofluid with smaller particles was found to be greater than that of the nanofluid with larger particles. It was also found that as particle concentration and flow rate rose, the average HTC value increased [25]. The HTC of nanofluids is raised by particle volume concentration, Brownian motion, and aspect ratio of nanoparticles similar to the flow Reynolds number, however particle diameter has the reverse impact. Furthermore, the kind of base fluid and nanoparticle have a considerable impact on the heat transfer characteristics of nanofluids. [26]

Chapter - 3: Geometry, Model and Computational Domain

3.1 Introduction

A numerical study was carried to perform a comparative study on HTC of Graphene nanoparticle (GnP) nanofluid and Multiwalled Carbon nanotube (MWCnT) nanofluid. In this chapter the geometry and modelling of the experimental setup and generation of computational domain will be discussed.

3.2 Geometry and Modelling

3.2.1 Heat Exchanger Details

In the experiment a U-shaped Concentric Tube in Tube Annulus Heat Exchanger was used. The model of the heat exchanger is Armfield HT31. It is a computer-controlled heat exchanger. Figure 2 represents the heat exchanger used in the experiment. The outer tube of the heat exchanger is constructed of acrylic and the inner tube is constructed of stainless steel.

The total heat transfer length is 660mm, where length of each leg of the U-shape is 330mm. The outer diameter of the acrylic tube (outer tube) is 12mm, and the outer diameter of the stainless-steel tube (inner tube) is 9.5mm. The wall thickness of the acrylic and steel tube are 0.3mm and 0.6mm respectively. Table 1 contains the values of geometric parameters of the Heat Exchanger.

Table 1: Geometric Parameters of Armfield HT31 Heat Exchanger

Geometric parameter	***Value (mm)***
Total Length	660
Outer Tube	
d_o	12
d_i	11.4
t	0.3
Inner Tube	
d_o	9.5
d_i	8.3
t	0.6

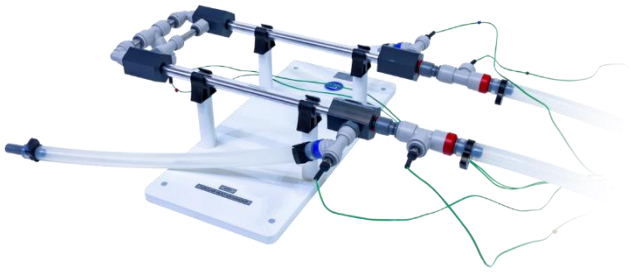

Figure 2: Armfield HT31 Heat Exchanger

3.2.2 Geometry and Model

A geometry is created to replicate the Heat Exchanger environment for generating the computational domain. In this section the formation of geometry and model along with their dimensions will be discussed in details.

The total length of either tube along which heat transfer will take place is 660mm. But the effective length will be 658.8mm. In Table 2 L_e is the effective length of one leg of the tube along which heat transfer will occur. The model contains three separate domains. The outer domain represents water domain, the inner domain represents nanofluid domain and the domain between water domain and nanofluid domain represents the steel tube through which heat transfer from hot fluid to cold fluid will occur.

Both the nanofluid domain and the steel tube has two bends due to the U-shape (Figure *6*, Figure *7*) and the water domain has four bends. The additional two bends are at the inlet and the outlet of the water domain. In the heat exchanger which was used in the experiment (Figure 6, Figure 7), the motion of water at entry and exit is perpendicular to the motion of nanofluid at its entry and exit. The additional two bends of the water domain satisfy this condition. Due to these additional bends in the water domain 0.6mm of length is reduced form each leg which results in the effective length (L_e) of each leg as 329.4mm.

The diameter of the nanofluid domain is 8.3mm which is the inner diameter of the inner (steel) tube. The water domain is annulus. Inner diameter of the water domain is 9.5mm, which is the outer diameter of the inner (steel) tube and the outer diameter of the water domain is 11.4mm which is the inner diameter of the outer (acrylic) tube. The total heat

transfer area is 0.019m^2. Table 2 contains the geometric parameters of the model and their values.

Table 2: Geometric Parameters of the Model

Geometric parameter	***Value (mm)***
L_e	329.4
$d_{w,o}$	11.4
$d_{w,i}$	9.5
d_{nf}	8.3
$d_{tube,o}$	9.5
$d_{tube,i}$	8.3

The model excludes the outer tube, as the heat transfer takes place between the two fluids through the inner (steel) tube. Outer (acrylic) tube takes no part in heat transfer. The exclusion of the outer tube reduces the computational time for analysis.

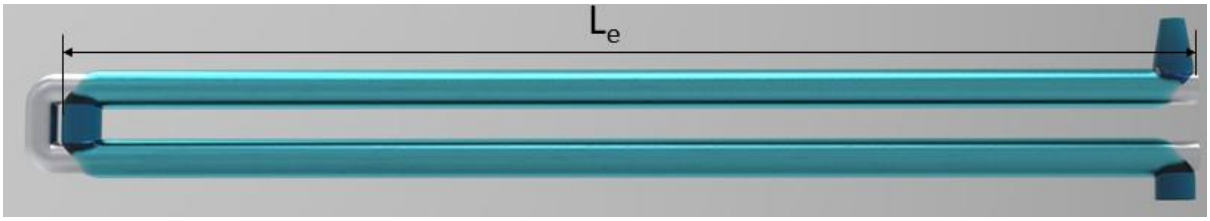

Figure 3: Schematic of U-shape Tubular Heat Exchanger model (front view)

Figure 3 represents the schematic of the heat exchanger model which will be used to generate the computational domain. It has two flow domains, i.e., water domain and nanofluid domain, and one solid domain, i.e., inner tube.

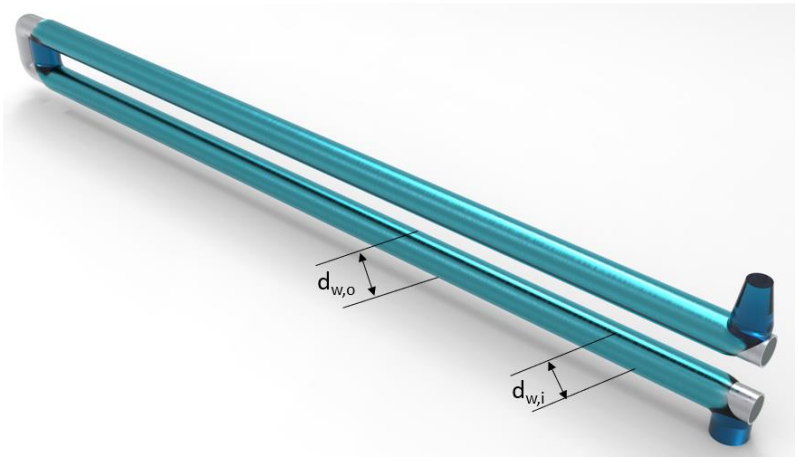

Figure 4: Schematic of U-shape Tubular Heat Exchanger

The Heat Exchanger is counter flow; the flow of water and nanofluid is opposite to each other. The inlet of water is of cylindrical shape, whereas the outlet is of conical shape (Figure 6). The outlet is made conical to avoid reverse flow in flow simulation. The shape of inlet and outlet of water doesn't affect the results of numerical analysis.

The regions between the legs of the U-shape of both water domain and nanofluid domain are not thermally connected hence, they don't participate in the heat transfer (Figure 3, Figure 6). The extended region of nanofluid domain in both sides also don't participate in heat transfer. Therefore, these regions are excluded from the effective length (L_e). These additional and extended regions are kept optimum by lessening them to a length which will not affect the mixing of the fluid layers at the bends. This reduces the number of mesh elements in the computational domain and eventually reducing the computational time without affecting the results of the numerical analysis. It is to be noted that at the bends the fluid layer mixes which distributes heat among the mixing layers.

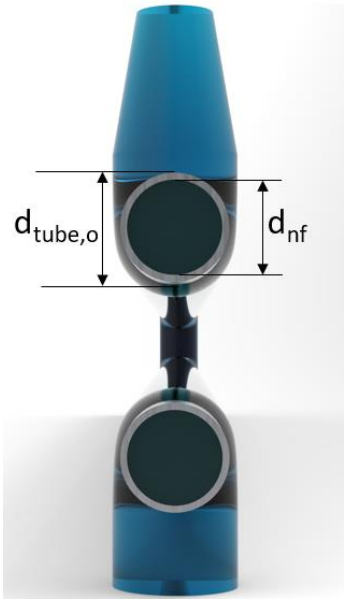

Figure 5: Schematic of U-shape Tubular Heat Exchanger (front view)

Figure 6: Water and Nanofluid domain (side view)

The inner tube is divided into three regions. Materials of two of these regions are steel and the third region is acrylic. The third region is an extended portion which doesn't participate in heat transfer between the fluids.

Figure 7: Steel tube

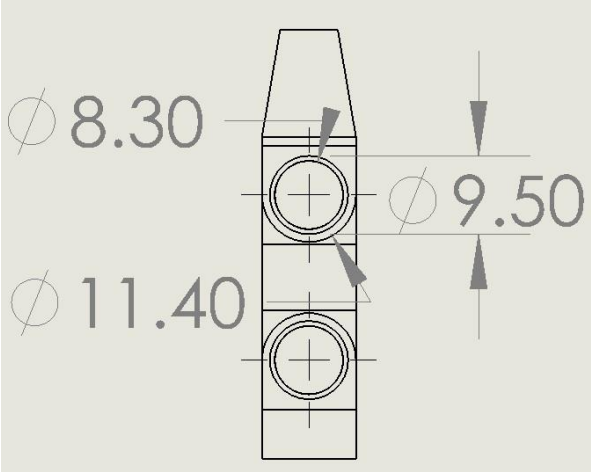

Figure 8: Schematic of the model (with dimensions)

3.3 Computational Domain

The model is created in CAD software Solidworks 2018. The mesh for the domain is generated in the simulation software ANSYS 2021.

The computational domain has three different sections, i.e., water flow domain, nanofluid flow domain, and inner tube domain. The three different domains have different mesh properties. Due to complex shape of the model unstructured mesh is used in all three domains. The mesh element shape is tetrahedral. The element size is different for the different domains. *Table 3* contains the mesh properties of the domain. Element size of water domain, nanofluid domain and inner tube are 0.5mm, 0.7mm and 0.4mm respectively.

For better flow in the boundary layer of the flow domains inflation is used in both water domain and nanofluid domain. In both cases *Total Thickness* inflation type is used. The inflation properties are given in Table 3.

The number of elements of the computational domain is 7.7 million.

The maximum skewness of the grid is 0.9 and average skewness is 0.14. The skewness is greater at the bends if the domains.

The section view of the grid layout is shown in Figure 9, Figure 10, Figure 11.

Table 3: Mesh properties

Domain	*Element shape*	*Element size (mm)*	*Inflation type*	*Number of layers*	*Growth rate*	*Maximum thickness (mm)*
Water domain	Tetrahedron	0.5	Total thickness	10	1.02	0.5
Nanofluid domain	Tetrahedron	0.7	Total thickness	10	1.05	2
Inner tube	Tetrahedron	0.4	-	-	-	-

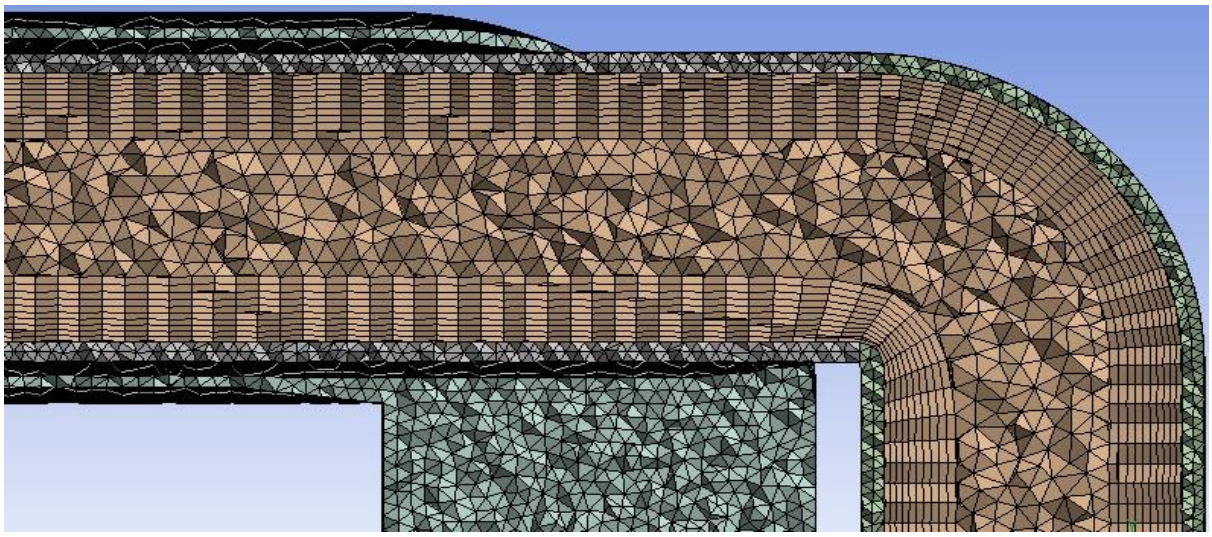

Figure 9: Grid layout of the domain at bend

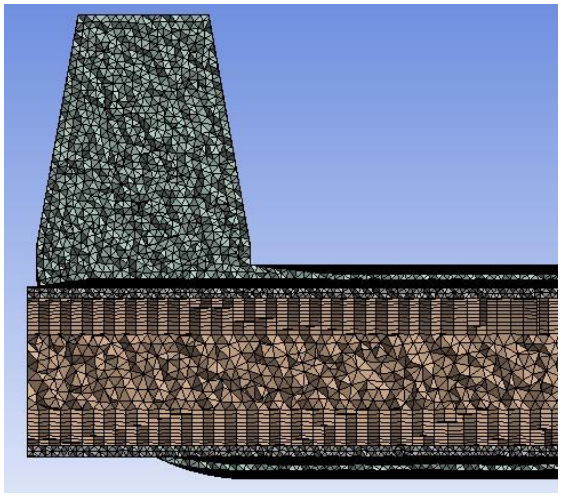

Figure 10: Grid layout of domain

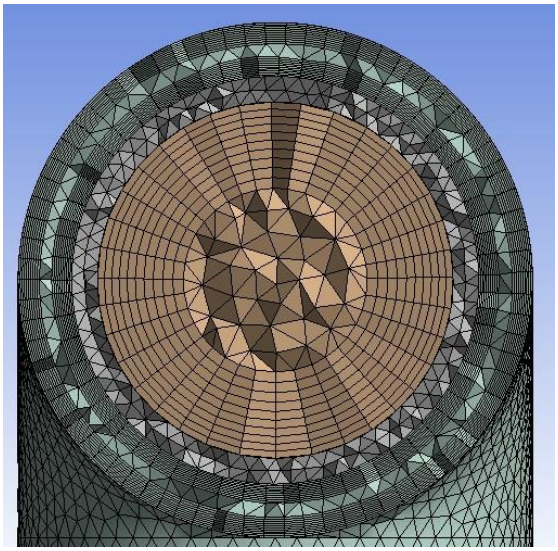

Figure 11: Grid layout of domain

Chapter - 4: Mathematical Formulation and Fluid Properties

4.1 Introduction

In this chapter the governing equations of Computational Flow Dynamics (CFD) Boundary Conditions and the mathematical correlations that were used in the numerical analysis will be discussed. For the analysis SST k-ω turbulence model is used. It's a two-equation turbulence model which is based on Reynold's Average Navier Stokes (RANS) equations. RANS equations are primarily used to describe turbulent flows.

The fluid properties of the both the fluids which are temperature dependent are to be calculated for their specific temperatures. The properties of nanofluid also vary with the concentration of nanofluid. Several correlations are used for this purpose. These will be discussed later in this chapter.

4.2 Governing Equations

Due to the flow properties of the fluid turbulent model is used in the numerical study. For this purpose, SST k-ω turbulent model is selected. SST k-ω is a two-equation eddy-viscosity model which is based on RANS equations. RANS equations are time averaged equation of the flow. In this model for the calculation of turbulence additional two equations are solved, i.e., kinetic energy and dissipation energy of eddies. Eddy viscosity models ere formulated based on the formation of eddies and dissipation of energy from the eddies.

Navier-Stokes equations are the governing equations of Computational Fluid Dynamics (CFD). These equations describe the flow of Newtonian Fluids for incompressible flow.

The governing equations of CFD for 3-dimensional incompressible flow for Newtonian fluid are as follows:

Continuity Equation:

$$\frac{\partial u}{\partial x} + \frac{\partial v}{\partial y} + \frac{\partial w}{\partial z} = 0 \quad (1)$$

Momentum Equations:

$$\rho \left(\frac{\partial u}{\partial t} + u\frac{\partial u}{\partial x} + v\frac{\partial u}{\partial y} + w\frac{\partial u}{\partial z} \right) = \rho g_x - \frac{\partial p}{\partial x} + \mu \left(\frac{\partial^2 u}{\partial x^2} + \frac{\partial^2 u}{\partial y^2} + \frac{\partial^2 u}{\partial z^2} \right) \quad (2)$$

$$\rho \left(\frac{\partial v}{\partial t} + u\frac{\partial v}{\partial x} + v\frac{\partial v}{\partial y} + w\frac{\partial v}{\partial z} \right) = \rho g_y - \frac{\partial p}{\partial y} + \mu \left(\frac{\partial^2 v}{\partial x^2} + \frac{\partial^2 v}{\partial y^2} + \frac{\partial^2 v}{\partial z^2} \right) \quad (3)$$

$$\rho \left(\frac{\partial w}{\partial t} + u\frac{\partial w}{\partial x} + v\frac{\partial w}{\partial y} + w\frac{\partial w}{\partial z} \right) = \rho g_z - \frac{\partial p}{\partial z} + \mu \left(\frac{\partial^2 w}{\partial x^2} + \frac{\partial^2 w}{\partial y^2} + \frac{\partial^2 w}{\partial z^2} \right) \quad (4)$$

Energy Equations:

$$\rho \frac{DE}{Dt} = \frac{\partial}{\partial x}\left[k\frac{\partial T}{\partial x}\right] + \frac{\partial}{\partial y}\left[k\frac{\partial T}{\partial y}\right] + \frac{\partial}{\partial z}\left[k\frac{\partial T}{\partial z}\right] - \frac{\partial (up)}{\partial x} - \frac{\partial (vp)}{\partial y} - \frac{\partial (wp)}{\partial z} + \Phi \quad (5)$$

here,

u = velocity component in x-direction

v = velocity component in y-direction

w = velocity component in z-direction

k = thermal conductivity

T = temperature

t = time

p = pressure

ρ = density

Φ = Dissipation Function (describes the effect of viscous stress)

4.3 Boundary Conditions

In this numerical study two fluids are used in each cased. Heat transfers from the nanofluid to water. Here nanofluid is considered as hot fluid and water is used as cold fluid. The flow rate of water is 1L/min. For each nanoparticle, three flowrates are used for nanofluids, i.e., 1.5L/min, 2L/min and 2.5L/min. For each flow rate five volume concentrations of nanoparticles are used, i.e., 0.01%, 0.05%. 0.15%. 0.25% and 0.35%. therefore, the total cases for validation is thirty. Table 4,

Table 5 and

Table 6 contains the mass flow rates of GnP nanofluids and Table 8 and

Table 9 contains the mass flow rates of MWCnT nanofluids for the three flowrates and five volume concentrations of nanoparticle.

The inlet temperature of water is 300K and the inlet temperature of nanofluids is 323K for all 30 cases. The gauge pressure is 0 for inlet and outlet of both fluids for all cases.

Table 4: Mass flow rate of GnP nanofluid for 1.5L/min flowrate

sl	***Flow rate***	***Volume concentration (%)***	***Mass flow rate (kg/s)***
1		0.01	0.024750750
2		0.05	0.024762851
3	1.5 L/min	0.15	0.024793103
4		0.25	0.024823356
5		0.35	0.024853608

Table 5: Mass flow rate of GnP nanofluid for 2L/min flowrate

sl	***Flow rate***	***Volume concentration (%)***	***Mass flow rate (kg/s)***
1		0.01	0.033001000
2		0.05	0.033017135
3	2 L/min	0.15	0.033057471
4		0.25	0.033097808
5		0.35	0.033138144

Table 6: Mass flow rate of GnP nanofluid for 2.5L/min flowrate

sl	*Flow rate*	*Volume concentration (%)*	*Mass flow rate (kg/s)*
1		0.01	0.041251250
2		0.05	0.041271419
3	2.5 L/min	0.15	0.041321839
4		0.25	0.041372259
5		0.35	0.041422680

Table 7: Mass flow rate of MWCnT nanofluid for 1.5L/min flowrate

sl	*Flow rate*	*Volume concentration (%)*	*Mass flow rate (kg/s)*
1		0.01	0.0249555048
2		0.05	0.0249715242
3	1.5 L/min	0.15	0.0250115727
4		0.25	0.0250516212
5		0.35	0.0250916697

Table 8: Mass flow rate of MWCnT nanofluid for 2L/min flowrate

sl	*Flow rate*	*Volume concentration (%)*	*Mass flow rate (kg/s)*
1		0.01	0.0332740064
2		0.05	0.0332953656
3	1.5 L/min	0.15	0.0333487636
4		0.25	0.0334021616
5		0.35	0.0334555596

Table 9: Mass flow rate of MWCnT nanofluid for 2.5L/min flowrate

sl	*Flow rate*	*Volume concentration (%)*	*Mass flow rate (kg/s)*
1		0.01	0.041592508
2		0.05	0.041619207
3	1.5 L/min	0.15	0.0416859545
4		0.25	0.0417527020
5		0.35	0.0418194495

4.4 Mathematical Formulation

The thermal properties, i.e., density, specific heat, thermal conductivity and dynamic viscosity of water and nanofluids and temperature dependent. Correlations are used to determine the values of these properties.

The thermal conductivity is determined using Maxwell model [27]. Gao et al. have determined the thermal conductivity of GnP nanofluids for volume concentration from 0.01% to 0.045% at 323K and found similarity with the maxwell correlation [27].

The Maxwell correlation for thermal conductivity of nanofluid is:

$$k_{nf} = \frac{k_p + 2k_f + 2\phi(k_p - k_p)}{k_p + 2k_f - \phi(k_p - k_p)}\, k_f \tag{6}$$

Corcione has developed a correlation for dynamic viscosity for both ethylene glycol based and water based nanofluids for a wide range of data [28]. The results of the empirical correlation have 1.84% standard deviation with the experimental data.

The correlation used for dynamic viscosity of nanofluid is:

$$\frac{\mu_{eff}}{\mu_f} = \frac{1}{1 - 34.87(d_p/d_f)^{-0.3}\varphi^{1.03}} \tag{7}$$

Maiga et al. have performed experiments on water and ethylene glycol based nanofluids. With wide range of data for different volume concentration in turbulent regime. They have developed a temperature dependent correlation for the thermal conductivity of water in turbulent regime [29].The correlation used to determine the thermal conductivity of water is:

$$k_f = 0.6067\left(-1.26523 + 3.704\left(\frac{T_{avg}}{298.15}\right) - 1.43955\left(\frac{T_{avg}}{298.15}\right)^2\right) \tag{8}$$

For turbulent regime the following correlation for dynamic viscosity is used [30] :

$$\mu_f = 2.414 \text{ x } 10^{-5} \text{ x } 10^{247.8/(T_{avg}-140)} \tag{9}$$

To determine density of water the following temperature dependent correlation is used [31]:

$$\rho_f = -3 \text{ x } 10^{-3} \, {T_{avg}}^2 + 1.505 T_{avg} + 816.781 \tag{10}$$

To determine specific heat the following temperature dependent correlation is used [31]:

$$C_{pf} = -4.63 \text{ x } 10^{-5} {T_{avg}}^3 + 0.0552 \, {T_{avg}}^2 - 20.86 T_{avg} + 6719.637 \tag{11}$$

The following correlation is used to determine the density of nanofluid for different volume concentration[32]:

$$\rho_{nf} = (1 - \phi)\rho_{bf} + \rho_{np} \tag{12}$$

The following correlation is used to determine the specific heat of nanofluid for different volume concentration [33]:

$$C_{p,nf} = \frac{(1 - \phi)\left(\rho C_p\right)_{bf} + \left(\rho C_p\right)_{np}}{\rho_{nf}} \tag{13}$$

The thermal properties of water are calculated for 300K and the thermal properties of nanofluids are calculated for 323K. The base-fluid of nanofluid is water. To determine the thermal properties of nanofluid, corresponding properties of base-fluid is to be determined. The temperature of base-fluid same as nanofluid, which is, 323K.

4.5 Thermal Properties of GnP nanofluid

The thermal properties whose variations are used in the study are density, specific heat, thermal conductivity and dynamic viscosity. These properties vary with both temperature and concentration. Properties are determined for the inlet temperature of fluids and for varying concentration.

4.5.1 Specific Heat

Figure 12 is the Specific Heat vs Volume Concentration curve for GnP nanofluid. The curve shows that as the volume concentration of nanoparticle increases the Specific Heat decreases. The maximum specific heat 4179.81kJ/kg/K, which occurs for 0.01% volume concentration. The specific heat continues to decrease after this point. The gradient of the graph in Figure *12* shows that the specific heat will continue to decrease as the volume concentration of GnP nanoparticle increases.

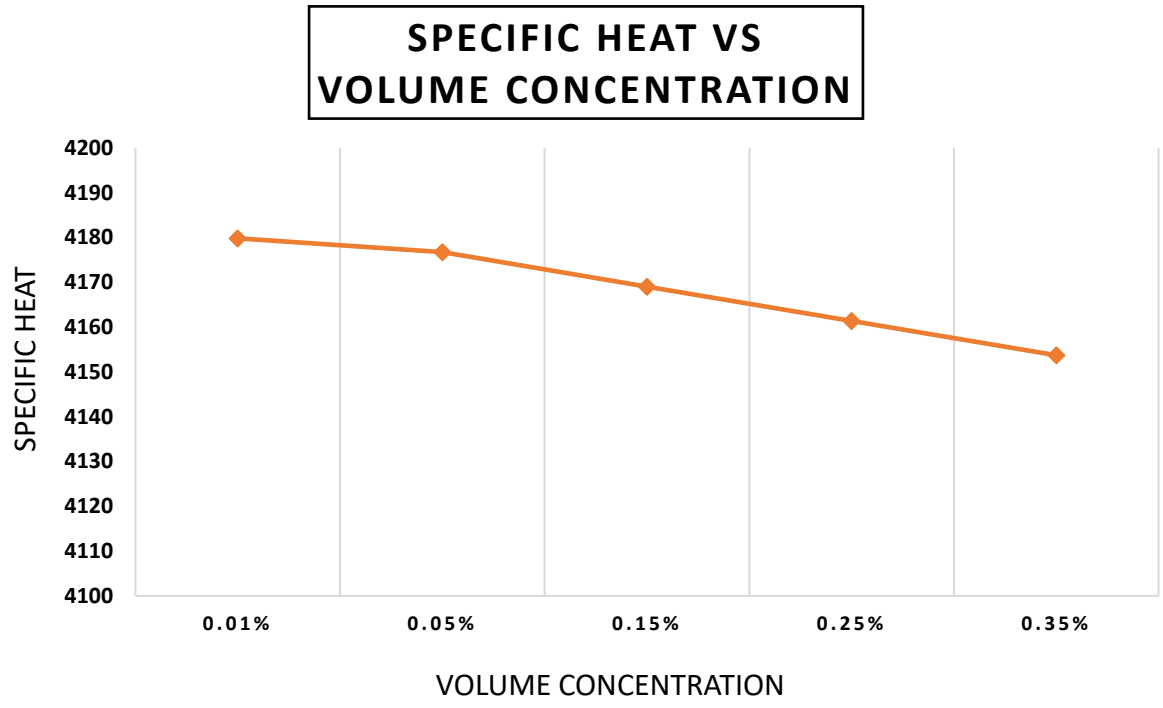

Figure 12: Specific Heat vs Volume Concentration curve for GnP nanofluid

4.5.2 Thermal Conductivity

Figure 13 is the Thermal Conductivity vs Volume Concentration curve for GnP nanofluid. The thermal conductivity of GnP nanofluid is 0.651517 W/m/K at 0.01% volume concentration. The maximum thermal conductivity occurred for the range 0.01% - 0.035% is 0.925042 W/m/K which occurred at 0.35% GnP volume concentration. The rise of thermal conductivity was slow in the beginning, but the rise became modest after 0.05% volume concentration. The gradient of the curve shows that the thermal conductivity will keep on rising as the volume concentration increases.

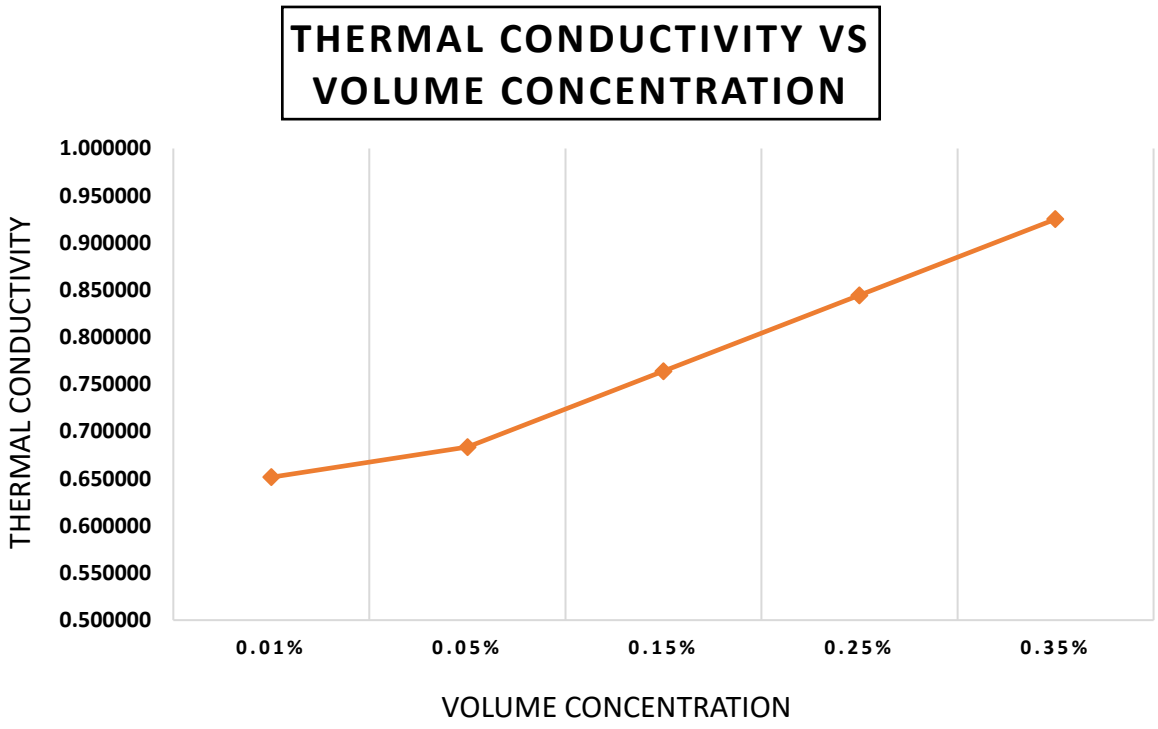

Figure 13: Thermal Conductivity vs Volume Concentration curve for GnP nanofluid

4.5.3 Dynamic Viscosity

Figure 14 has the Volume Concentration curve for GnP nanofluid. Dynamic viscosity increases with the increase of volume concentration. The minimum dynamic viscosity occurs at 0.0006677293 Pa-s which occurs for 0.01% volume concentration and the maximum dynamic viscosity is 0.001220691 Pa-s which occurs for 0.35% volume

concentration of GnP nanoparticle. The gradient of the curve shows that the dynamic viscosity will continue to rise as the volume concentration of GnP nanoparticles increases.

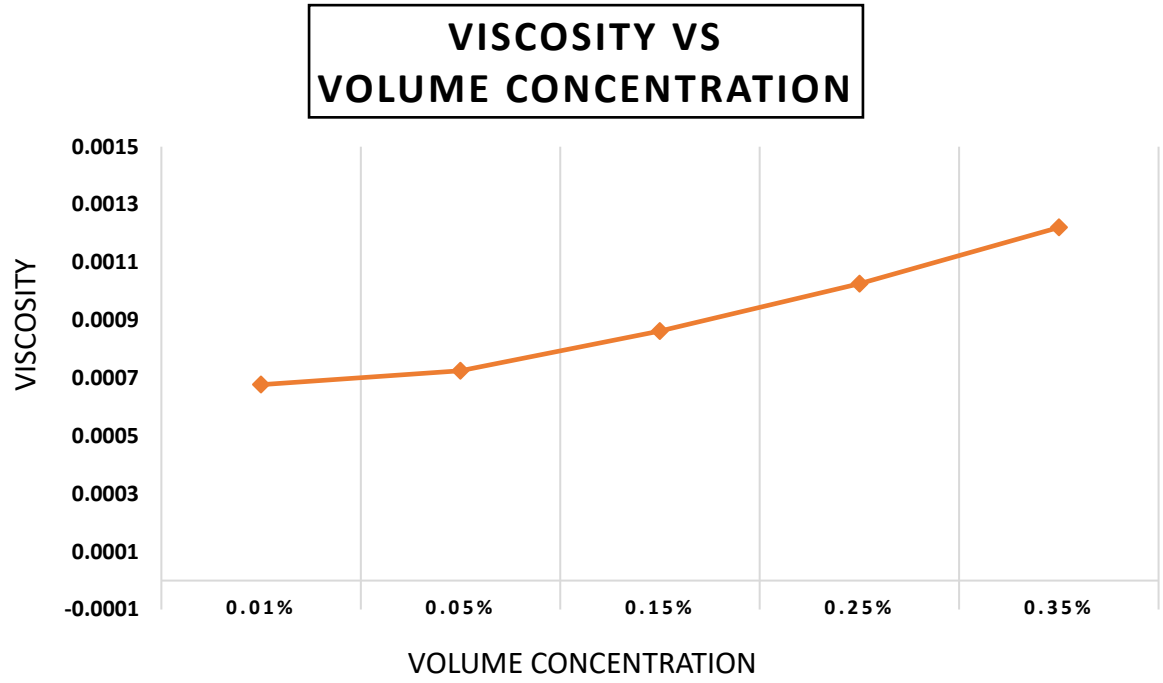

Figure 14: Dynamic Viscosity vs Volume Concentration curve for GnP nanofluid

4.6 Thermal Properties of MWCnT nanofluid

Likewise, the thermal properties of the GnP nanofluid, the thermal properties of the MWCnT nanofluids shows variations with the volume concentration of the MWCnT nanoparticles. The values for the following properties specific heat, thermal conductivity, dynamic viscosity have been calculated and described in the following sections.

4.6.1 Specific Heat

Figure *15* is the Specific Heat vs Volume Concentration curve for MWCnT nanofluid. The curve shows that as the volume concentration of nanoparticle increases the Specific Heat decreases. The maximum specific heat 4180.618kJ/kg/K, which occurs for 0.01% volume concentration. The specific heat continues to decrease after this point. The gradient of the graph in Figure *15* shows that the specific heat will continue to decrease as the volume concentration of MWnT nanoparticle increases.

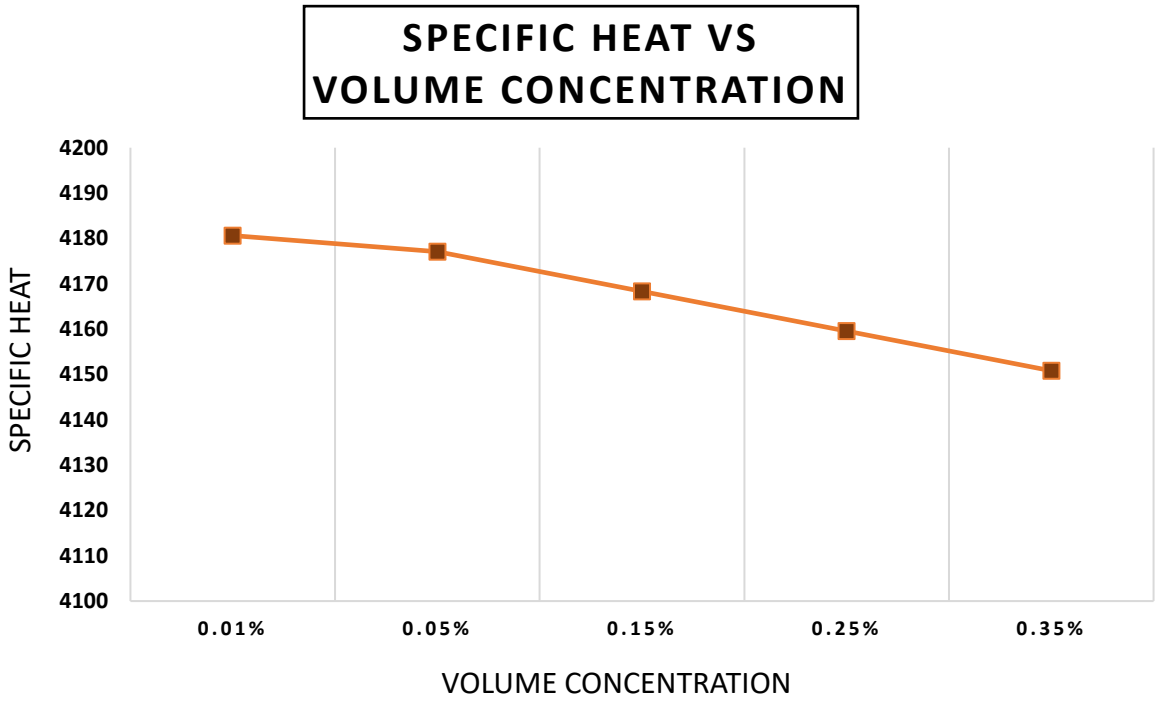

Figure 15: Specific Heat vs Volume Concentration curve for MWCnT nanofluid

4.6.2 Thermal Conductivity

Figure *16* is the Thermal Conductivity vs Volume Concentration curve for MWCnT nanofluid. The thermal conductivity of MWCnT nanofluid is 0.64369 W/m/K at 0.01% volume concentration. The maximum thermal conductivity occurred for the range 0.01% - 0.035% is 0.65027 W/m/K which occurred at 0.35% MWCnT volume concentration. The rise of thermal conductivity was slow in the beginning, but the rise became modest after 0.05% volume concentration. The gradient of the curve shows that the thermal conductivity will keep on rising as the volume concentration increases.

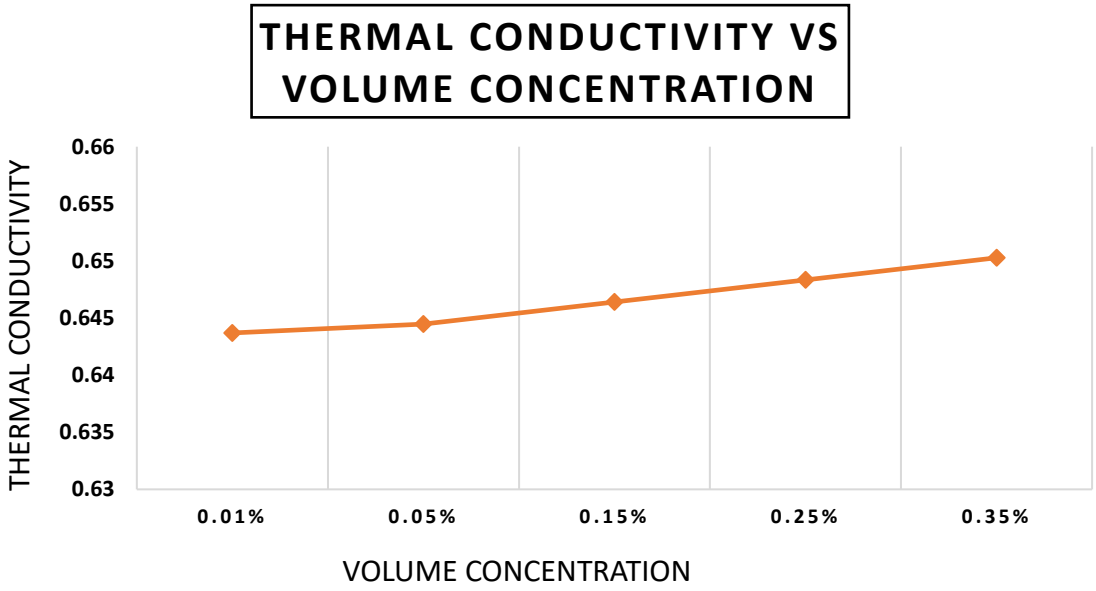

Figure 16: Thermal Conductivity vs Volume Concentration curve for MWCnT nanofluid

4.6.3 Dynamic Viscosity

Figure *17* has the Volume Concentration curve for MWCnT nanofluid. Dynamic viscosity increases with the increase of volume concentration. The minimum dynamic viscosity occurs at 0.000547 Pa-s which occurs for 0.01% volume concentration and the maximum dynamic viscosity is 0.000551 Pa-s which occurs for 0.35% volume concentration of MWCnT nanoparticle. The gradient of the curve shows that the dynamic viscosity will continue to rise as the volume concentration of MWCnT nanoparticles increases.

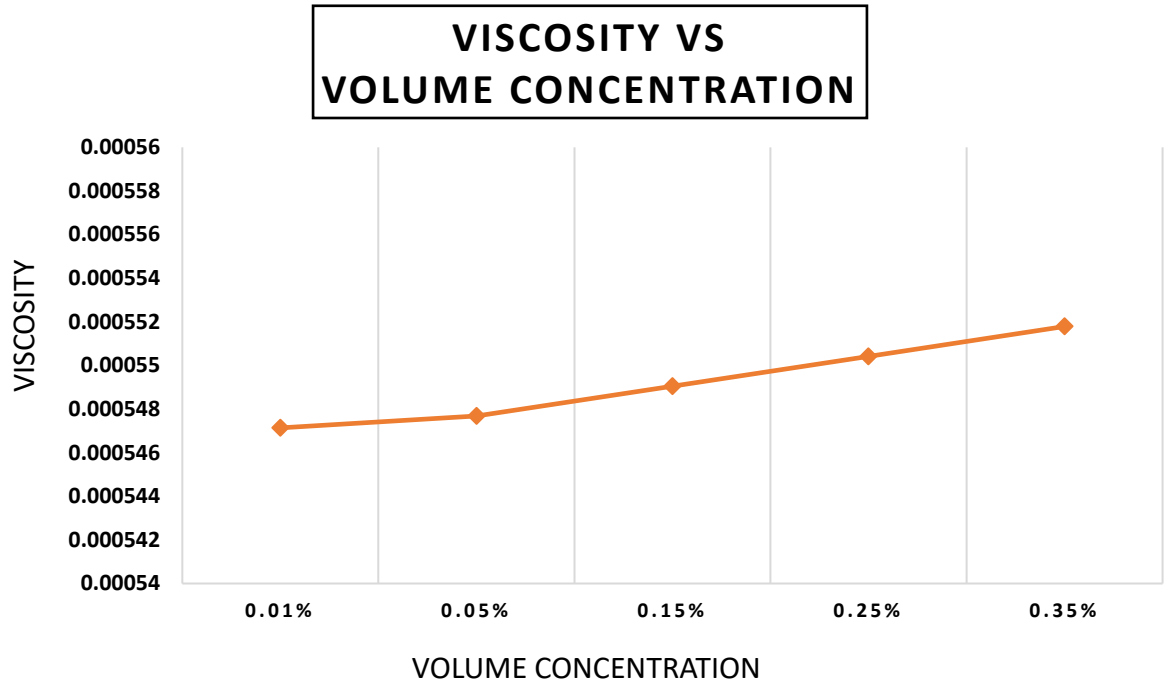

Figure 17: Dynamic Viscosity vs Volume Concentration curve for MWCnT nanofluid

Chapter - 5: Numerical Methodology

In this chapter the method and work flow of the study will be described in details.

The numerical study was performed using various software packages. For the CAD model generation Solidworks 2018 was used. The mesh was generated using ANSYS mechanical. The simulations were done in Ansys Fluent. For this purpose, Ansys 2020 software package was used.

5.1 Mesh Details and Grid Independence

The CAD model was imported to Ansys Mechanical in Parasolid form to generate mesh. Parasolid format is preferred for complex geometries with curved surfaces and complex edges. Several trial and error were done while refining the mesh. For the boundary layer of flow inflation was used to generate refined mesh. Unstructured mesh was used for the complexity of the geometry. The details of the mesh generation is given in the section *Geometry and Model.* Mesh quality plays a vital role in the result of flow analysis. The skewness of the generated mesh was kept low. The average skewness is 0.14 in the used mesh. The mesh element number is 7.7million.

Grid independence test was performed to determine the optimum mesh. Total seven grid was generated using different mesh element size. For each mesh simulation was run to determine the error of the result. To reduce error finer mesh was generated. The optimum grid was selected for fine mesh with acceptable error and for optimal computational time. Therefore, for this numerical analysis the 4^{th} grid in *Table 10* with 1.85% error in result was selected. The number of mesh element is 7.7million. The error was calculated for the HTC of GnP nanofluid for 1.5L/min flowrate for 0.01% volume concentration of nanoparticles.

Table 10: Grid independence data

Sl No	*Mesh Elements*	*Heat Transfer Co-efficient ($W/m^2/K$)*	*Error*
1	2490000	704.66	25.27%
2	4870000	836.87	14.1%
3	5950000	967.25	6.15%
4	7700000	1081.06	1.85%
5	8260000	1092.79	0.7%
6	10380000	1098.43	1.38%

5.2 Numerical Model and Schemes

Turbulence model is used for the numerical analysis. The type flow of the fluids is internal flow. The Reynolds number for turbulence regime for internal flow starts from 4000. The maximum Reynolds number among all the cases is 5205 and minimum is 3105. Though the minimum Reynolds number falls is transition regime, but due to the complexity of the geometry turbulence model works better.

SST k-ω model is used in the analysis. This is a two-equation eddy viscosity model. SST k-ω model combines the behaviour of both k-ω and k-ϵ models. The use of k-ω formulation in boundary layer makes the model directly usable from the boundary layer to the wall through the whole viscous sublayer. This model works for low Reynolds number without using damping functions. In free stream the model switches to k-ϵ model. A common problem of k-ω model is, it is too sensitive to inlet free stream turbulence properties. Thus, the SST k-ω turbulence model can avoid the common k-ω problem.

For pressure-velocity coupling SIMPLE (Semi-Implicit Method for Pressure-Linked Equations) was used. The Schemes used for Spatial Discretization is given in *Table 11*. Though Second Order upwind scheme prove more accurate result but it costs greater computational time. As the flow has low turbulence so for Turbulent Kinetic Energy and Specific Dissipation Rate First Order Upwind scheme was used. This caused insignificant error but the computational time decreased by a considerable amount.

Table 11: Spatial Discretization Schemes used in the Numerical Analysis

Field Variable	*Scheme*
Gradient	Least Square Cell Based
Pressure	Second Order
Momentum	Second Order Upwind
Turbulent Kinetic Energy	First Order Upwind
Specific Dissipation Rate	First Order Upwind
Energy	Second Order Upwind

5.3 Fluid Properties

Using the correlations provided in *Section 4.4* the fluid properties were calculated. The thermal properties of the fluids were plotted in Figure 12, Figure 13, Figure 14, Figure 15, Figure 16, Figure 17. The fluid properties are given in Table 12 and

Table 13.

Table 12: Properties of GnP Nanofluid

Sl no	***Flow rate***	***Volume concentration***	***Density***	***Specific Heat***	***Mass flow rate***	***Thermal Conductivity***	***Viscosity***
1	**1.5 L/min**	0.01%	990.03	4179.8168	0.02475075	0.651517	0.00068
2		0.05%	990.514	4176.7338	0.02476285	0.6836	0.00073
3		0.15%	991.7241	4169.0395	0.0247931	0.7639255	0.00086
4		0.25%	992.9342	4161.364	0.02482336	0.844405	0.00103
5		0.35%	994.1443	4153.7071	0.02485361	0.9250417	0.00122
6	**2 L/min**	0.01%	990.03	4179.8168	0.033001	0.651517	0.00068
7		0.05%	990.514	4176.7338	0.03301713	0.6836	0.00073
8		0.15%	991.7241	4169.0395	0.03305747	0.7639255	0.00086
9		0.25%	992.9342	4161.364	0.03309781	0.844405	0.00103
10		0.35%	994.1443	4153.7071	0.03313814	0.9250417	0.00122
11	**2.5 L/min**	0.01%	990.03	4179.8168	0.04125125	0.651517	0.00068
12		0.05%	990.514	4176.7338	0.04127142	0.6836	0.00073
13		0.15%	991.7241	4169.0395	0.04132184	0.7639255	0.00086
14		0.25%	992.9342	4161.364	0.04137226	0.844405	0.00103
15		0.35%	994.1443	4153.7071	0.04142268	0.9250417	0.00122

Table 13: Properties of MWCnT Nanofluid

Sl no	***Flow rate***	***Volume concentration***	***Density***	***Specific Heat***	***Mass flow rate***	***Thermal Conductivity***	***Viscosity***
1	**1.5 L/min**	0.01%	990.23	4180.618	.02495550485	0.643693	0.000547
2		0.05%	990.714	4177.094	.02497152425	0.644465	0.000548
3		0.15%	992.324	4168.303	.02501157275	0.646398	0.000549
4		0.25%	993.934	4159.54	.02505162125	0.648335	0.00055
5		0.35%	995.5443	4150.805	.02509166975	0.650276	0.000552
6	**2 L/min**	0.01%	990.23	4180.618	.03327400647	0.643693	0.000547
7		0.05%	990.714	4177.094	.03329536567	0.644465	0.000548
8		0.15%	992.324	4168.303	.03334876367	0.646398	0.000549
9		0.25%	993.934	4159.54	.03340216167	0.648335	0.00055
10		0.35%	995.5443	4150.805	.03345555967	0.650276	0.000552
11	**2.5 L/min**	0.01%	990.23	4180.618	.04159250808	0.643693	0.000547
12		0.05%	990.714	4177.094	.04161920708	0.644465	0.000548
13		0.15%	992.324	4168.303	.04168595458	0.646398	0.000549
14		0.25%	993.934	4159.54	.04175270208	0.648335	0.00055
15		0.35%	995.5443	4150.805	.04181944958	0.650276	0.000552

Each flow rate of each nanofluid has five cases for five different volume concentration of nanoparticle. So, there are total 30 cases for both nanofluids. The thermal properties depend on volume concentration of nanoparticles. So, the thermal properties have repeated for each volume concentration. Only the mass flow rate is unique for each case, as mass flow rate depends on both volume flow rate and density of the fluid. The combination of density and volume flow rate is unique for all each case.

These are the inlet properties of the fluid. The inlet temperature of nanofluid is 323K and water is 300K.

Chapter - 6: Result and Discussion

In this numerical study the experimental result done by *Dayou et al.* is validated. The experiment was done to determine and compare the HTC of GnP and MWCnT nanofluids.

The experiment was carried out for three flow rates. Nanofluids were prepared for five volumetric concentrations, i.e., 0.01%, 0.05%, 0.15%, 0.25% and 0.35%.

The nanofluids were prepared using two types of nanoparticles, i.e., Graphene nanoparticle and Multiwalled Carbon nanotube.

The following graphs are generated from the experimental results and numerical results of the given conditions. The graphs compare the HTCs for the different flowrates for experimental results and numerical results separately as well compare the HTCs from experimental results and numerical results for each flow rate.

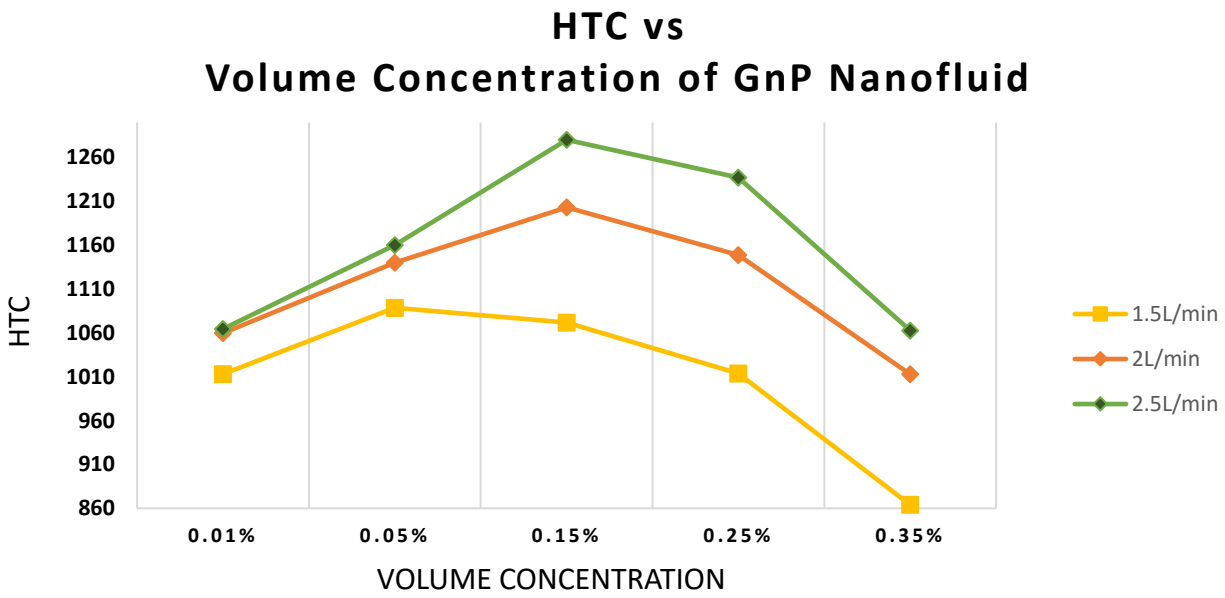

Figure 18: HTC of GnP nanofluid for 1.5L/min, 2L/min and 2.5L/min from the Experimental results by Dayou et. Al

Figure *18*, Figure *20* contains the graph of HTCs for the flow rates 1.5 L/min, 2 L/min and 2.5 L/min for the results from the experiment of Dayou et. Al. Figure *19*, Figure *21* is contains the graph for the results generated for the same cases of the experiment. Both experimental and the numerical analysis shows that the maximum HTC occurs for 2.5L/min flow rate of GnP nanofluid at 0.15% volume concentration.

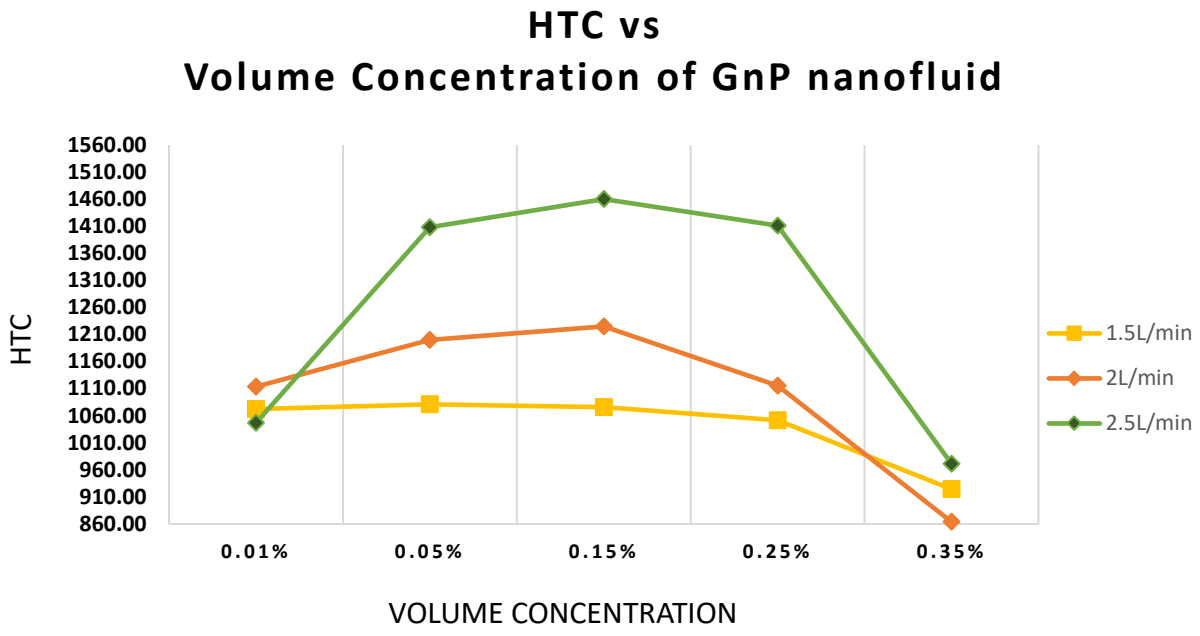

Figure 19: HTC of GnP nanofluid for 1.5L/min, 2L/min and 2.5L/min from the Numerical results

.

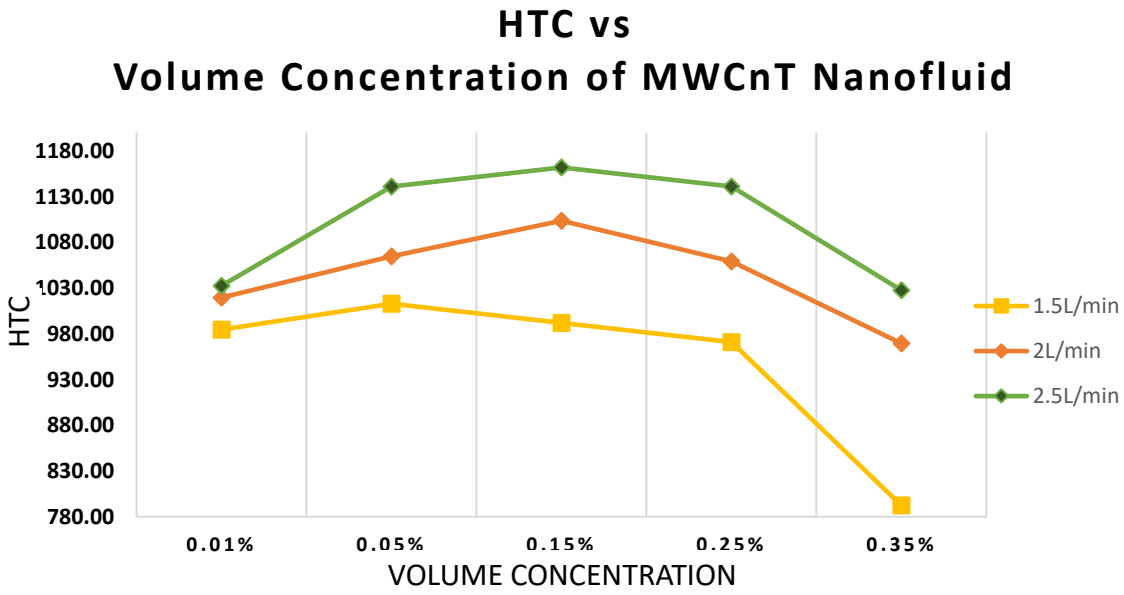

Figure 20: HTC of MWCnT nanofluid for 1.5L/min, 2L/min and 2.5L/min from the Experimental results by Dayou, Sebastian, Ting, Tiew Wei, Vigolo and Brigitte

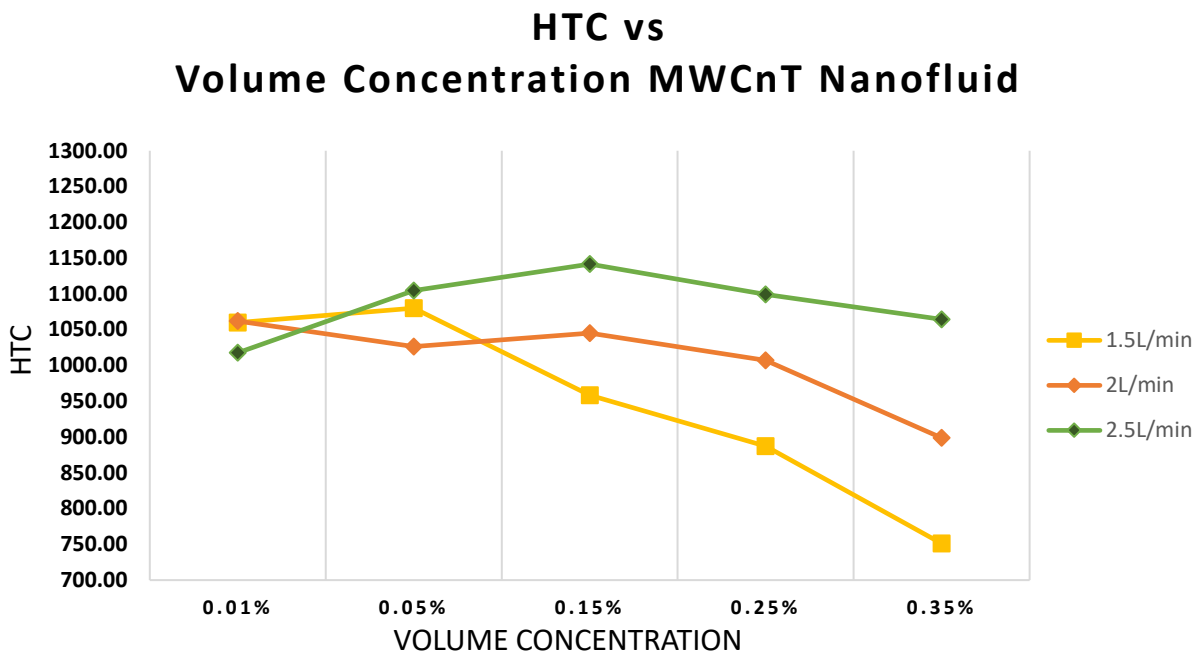

Figure 21: HTC of MWCnT nanofluid for 1.5L/min, 2L/min and 2.5L/min from the Numerical results

It is evident that the maximum HTC occurs at 2.5L/min flow rate for both nanofluid. Figure 22 compares the HTC of GnP nanofluid and MWCnT nanofluid for the given range of nanoparticle volume concentration. For both nanofluids the maximum HTC occurs for 0.15% volume concentration.

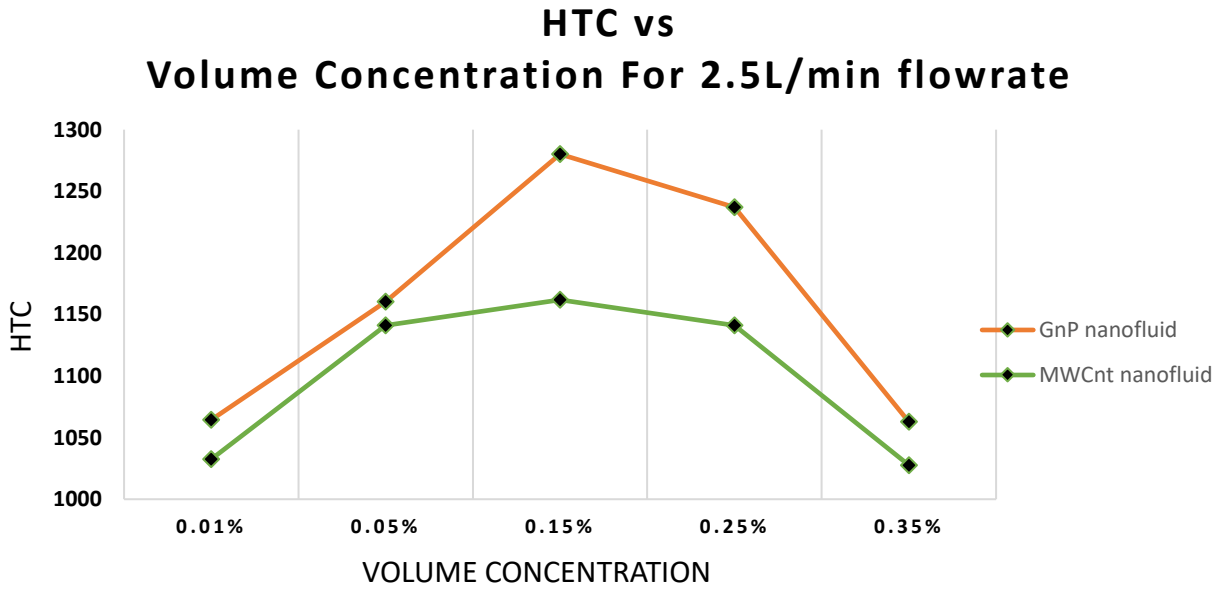

Figure 22: HTC of GnP nanofluid and MWCnT nanofluid for 2.5L/min flowrate from the experimental results

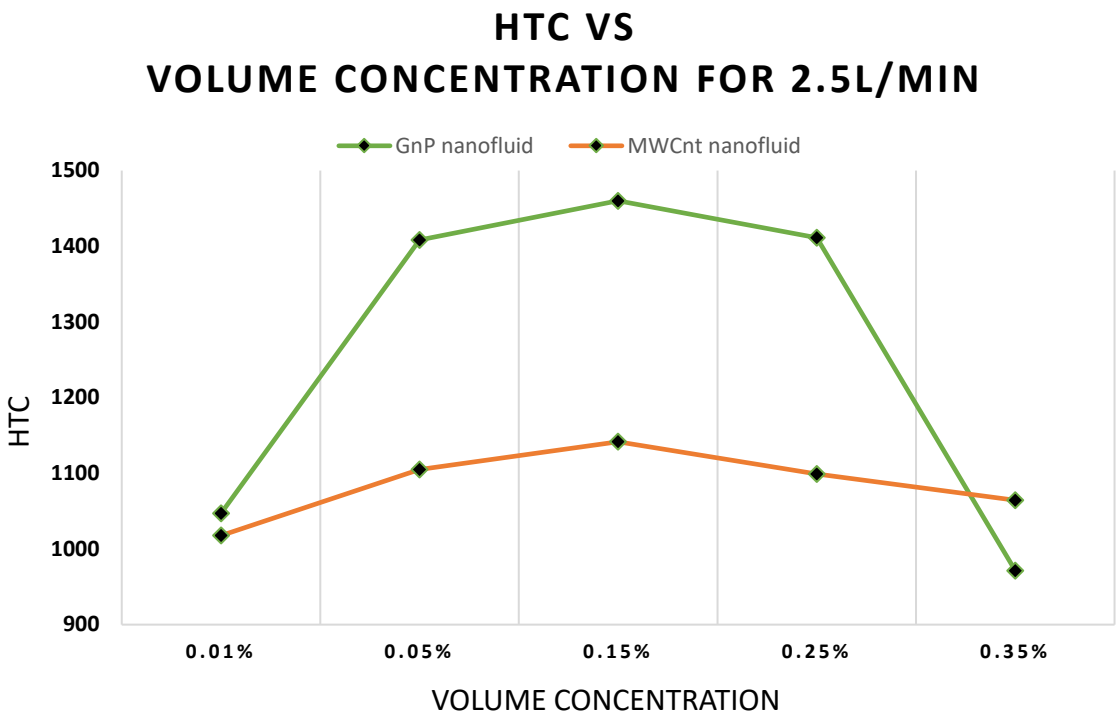

Figure 23: HTC of GnP nanofluid and MWCnT nanofluid for 2.5L/min flowrate from the numerical results

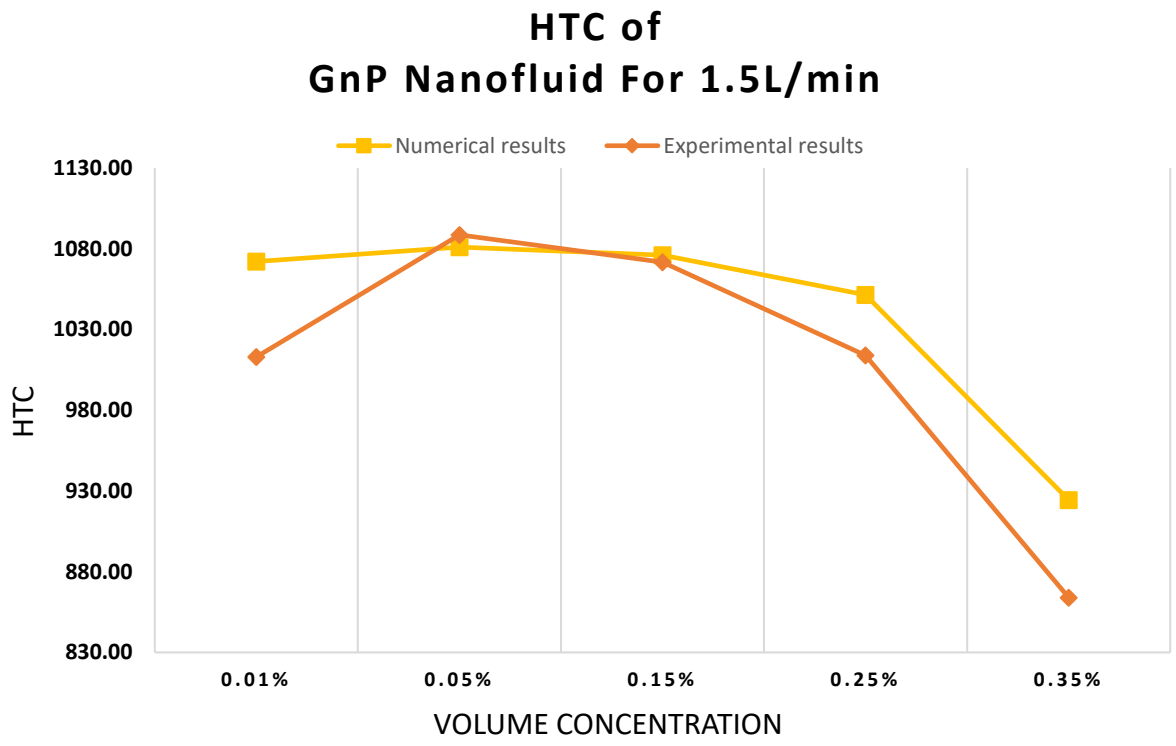

Figure 24: HTCs of GnP nanofluids for 1.5L/min from experimental and numerical results

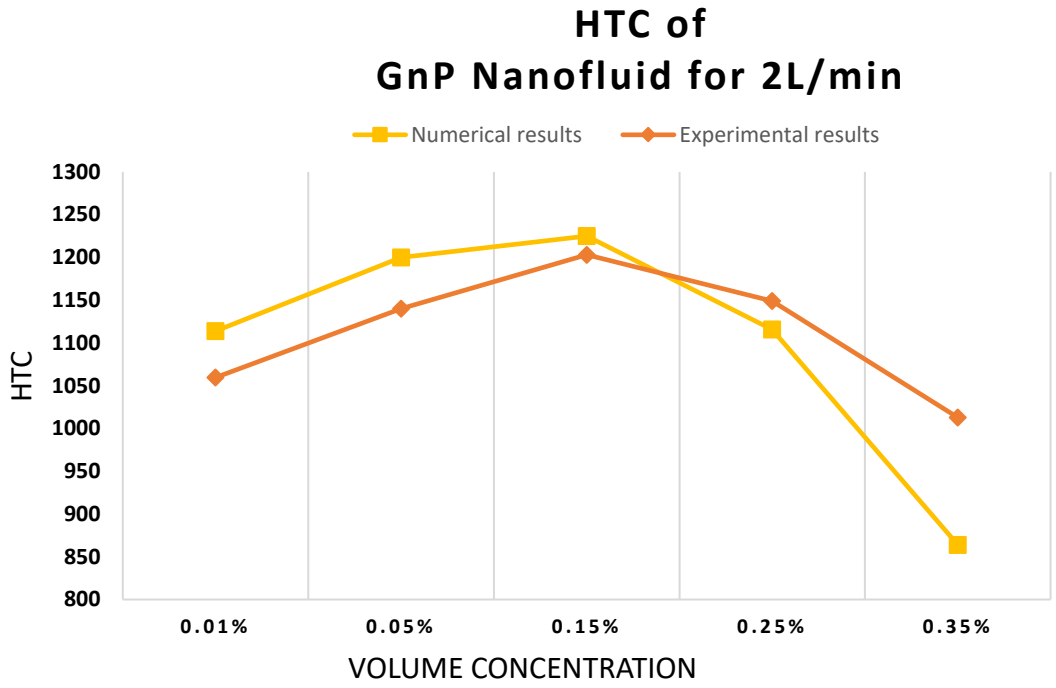

Figure 25: HTCs of GnP nanofluids for 2L/min from experimental and numerical results

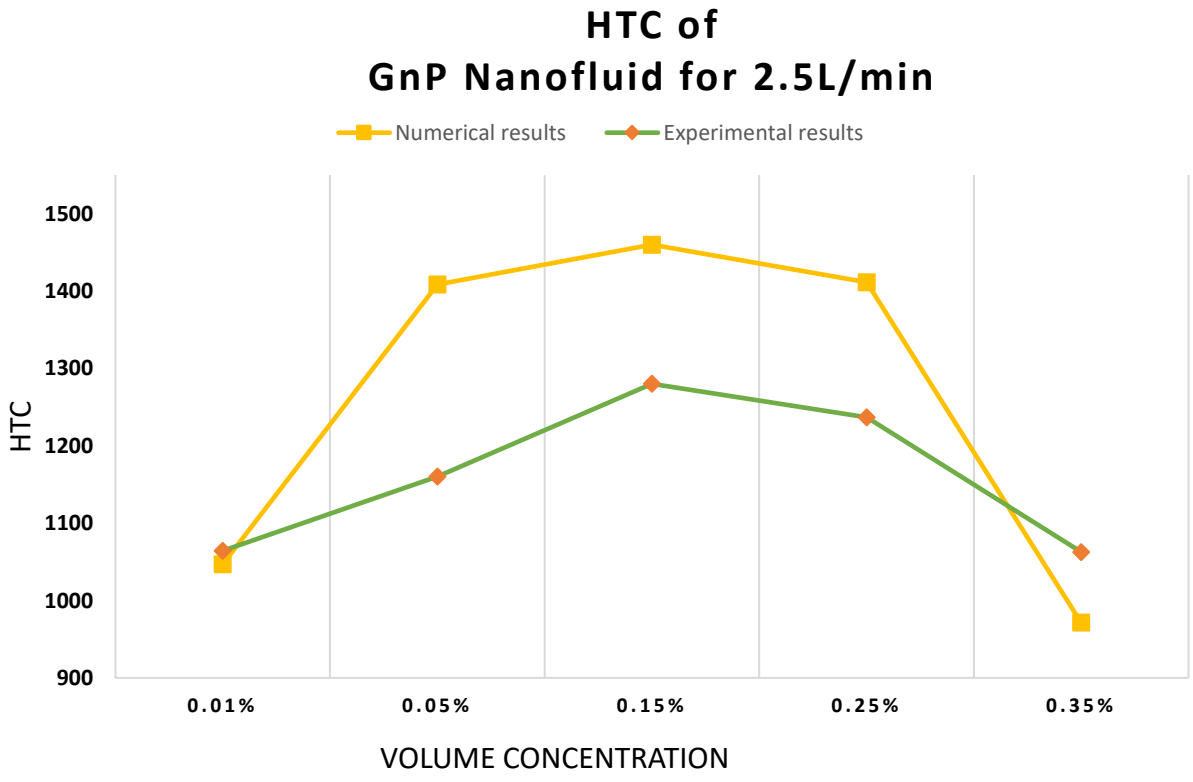

Figure 1-26: HTCs of GnP nanofluids for 2.5L/min from experimental and numerical results

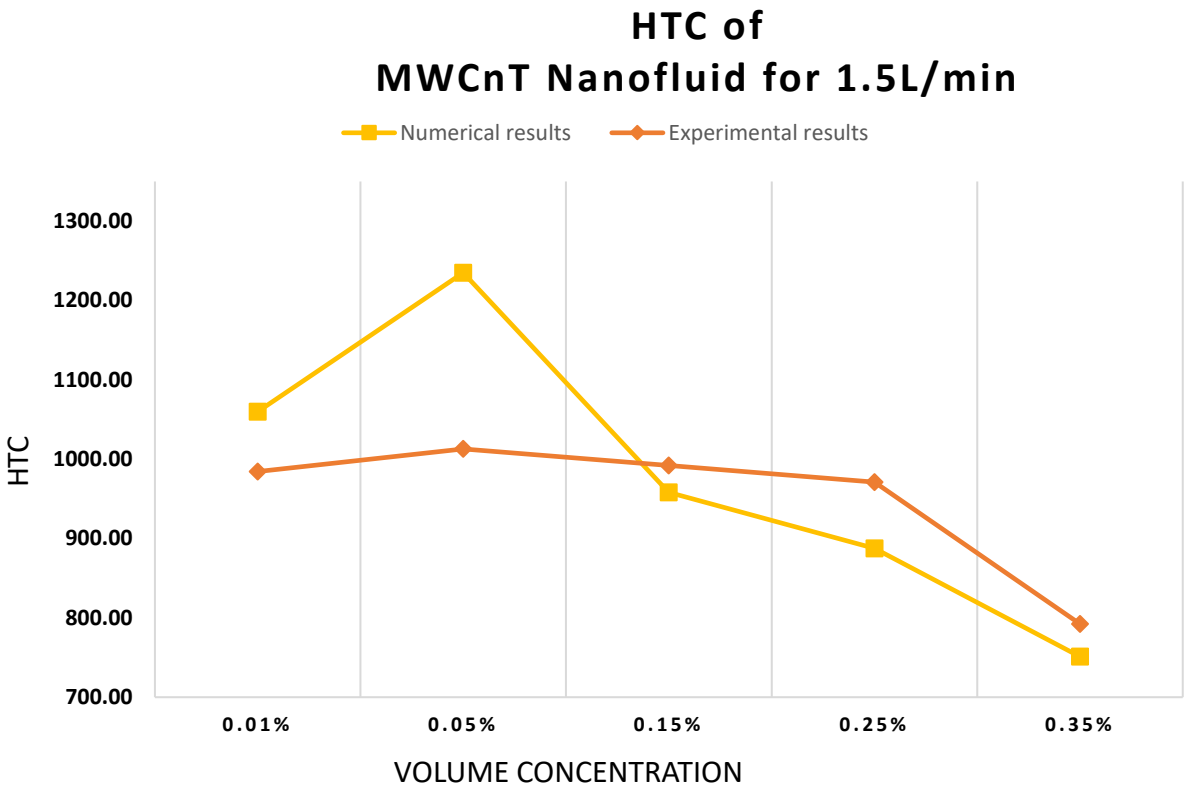

Figure 27: HTCs of MWCnT nanofluids for 1.5L/min from experimental and numerical results

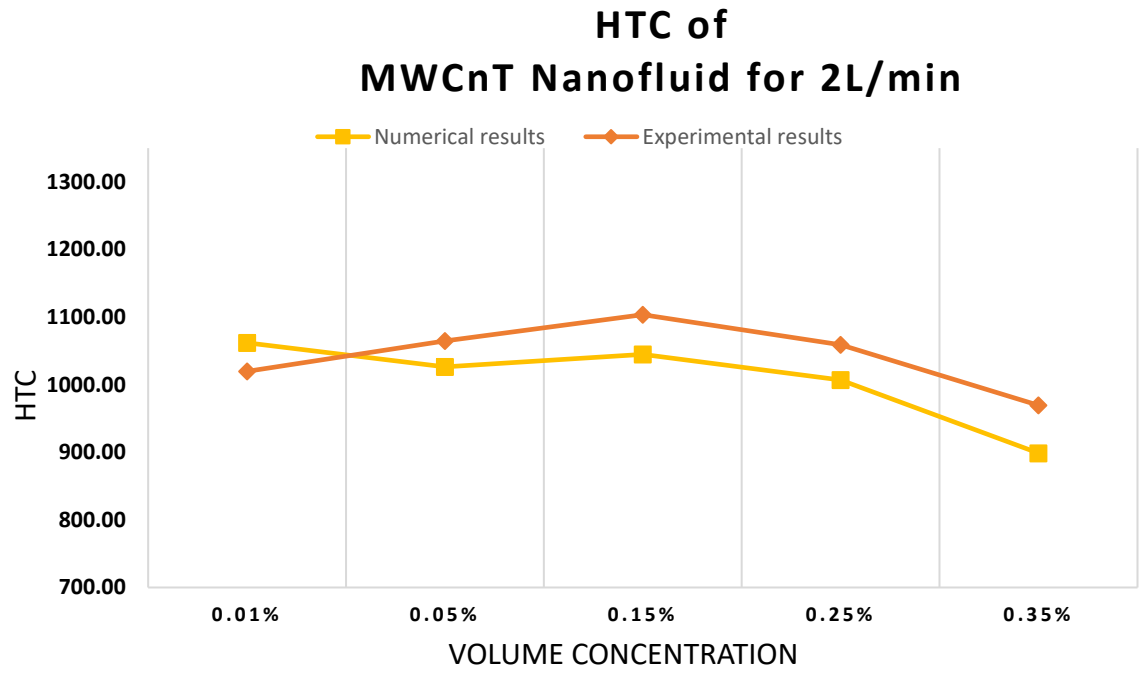

Figure 28: HTCs of MWCnT nanofluids for 2L/min from experimental and numerical results

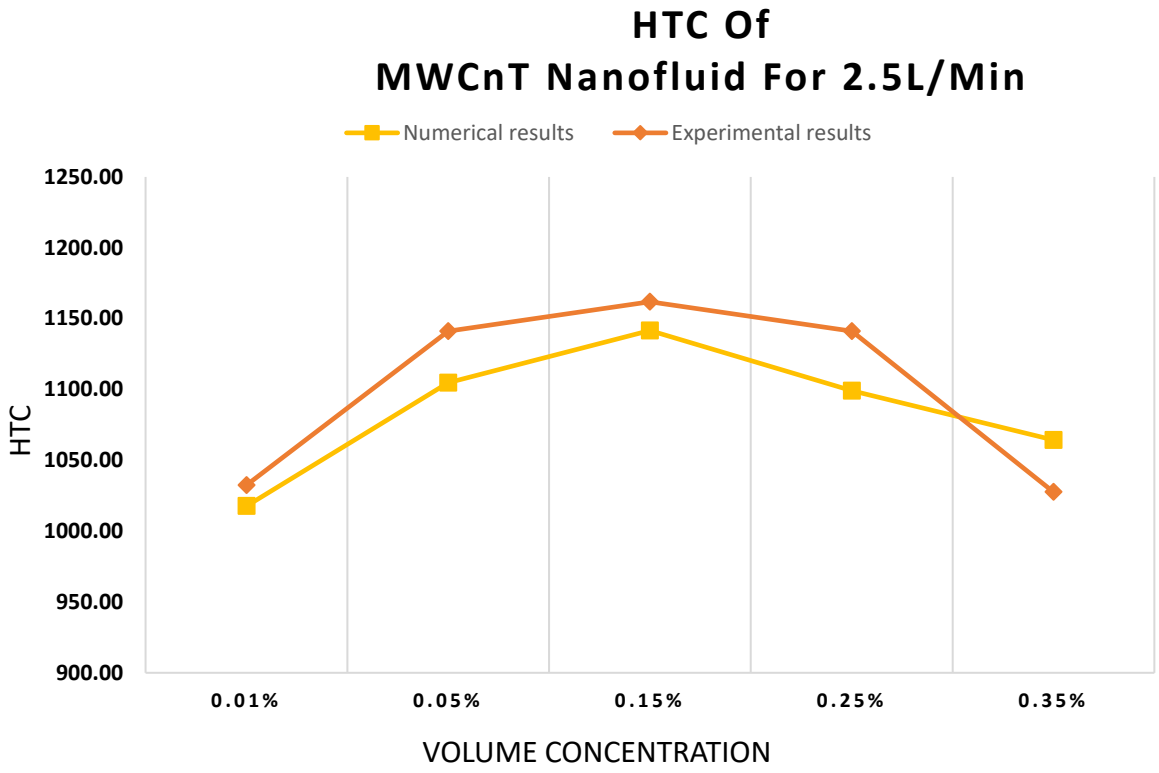

Figure 29: HTCs of MWCnT nanofluids for 2.5L/min from experimental and numerical results

For both GnP and MWCnT nanofluid for 1.5L/min flow rate the maximum heat coefficient was obtained for 0.05% nanoparticle concentration. It is to be noted that the volume concentration was considered while preparing nanofluid. For 2L/min and 2.5L/min flow rate the maximum HTCs was obtained at 0.15% nanoparticle concentration for both the nanofluids. For 1.5L/min flowrate the HTC starts to decrease after 0.05% nanoparticle concentration. For 2L/min and 2.5L/min flowrate the HTC starts to decrease after 0.15% nanoparticle concentration. The base fluid of the nanofluids is water. The specific heat of both GnP and MWCnT nanoparticles are lesser than water and the thermal conductivity is greater than water. So, HTC increases when the nanoparticle concentration in nanofluid increases. But it is observed that the HTC decreases after a certain volume concentration. When concentration of nanoparticles increases the thermal conductivity of nanofluid increases and specific heat of nanofluid decreases. Due to increase of nanoparticle concentration the dynamic viscosity of nanofluid also increases. The heat transfer in fluid is affected by Brownian motions,

clustering effect, thermophoresis, layering of liquid in molecular level at the liquid-solid interface, turbulence. Due to the increase in nanoparticle concentration the viscosity increases hence the mixing of layer is obstructed, clustering occurs as well the layering in liquid is affected. The structure of MWCnT creates greater thermal boundary layer. For both nanofluids the HTC is greater for 0.15% nanoparticle concentration at 2.5L/min flow rate. The HTC of GnP nanofluid is greater than MWCnT nanofluid at 0.15% nanoparticle concentration at 2.5L/min. Hence, it can be concluded that Graphene nanoparticle provides better performance.

Chapter - 7: Conclusion

In this study a numerical study has been done to compare the HTC of GnP nanofluid and MWCnT nanofluid. The greatest HTC was found to be achieved with 0.05 percent nanoparticle concentration for both GnP and MWCnT nanofluids operating at a flow rate of 1.5 litres per minute. When producing the nanofluid, it is important to notice that the volume concentration was taken into consideration. At a nanoparticle concentration of 0.15 percent for both nanofluids, the greatest HTCs were found for flow rates of 2 litres per minute and 2.5 litres per minute, respectively. Once there is a concentration of 0.05 percent nanoparticles, the HTC begins to drop with a flowrate of 1.5 litres per minute. After a nanoparticle concentration of 0.15 percent, the HTC begins to decline for flowrates of 2 litres per minute and 2.5 litres per minute. Water serves as the foundational medium for the nanofluids. The thermal conductivity of GnP and MWCnT nanoparticles is higher than that of water, despite the fact that their specific heat values are lower than those of water. Therefore, a rise in the nanoparticle concentration in the nanofluid causes an increase in the HTC. However, once a specific volume concentration has been reached, it has been seen that the HTC begins to decline. The drop in specific heat of the nanofluid is accompanied by a rise in the thermal conductivity of the nanofluid when the concentration of nanoparticles is increased. The dynamic viscosity of the nanofluid will increase as a result of an increase in the concentration of nanoparticles. Brownian movements, the clustering effect, thermophoresis, layering of liquid on a molecular level at the liquid-solid interface, and turbulence are all factors that can impact the rate at which heat is transferred through a fluid. The rise in nanoparticle concentration causes an increase in viscosity, which results in the layer mixing being hindered, clustering occurring, and the layering in liquid being disrupted. Greater thermal boundary layer is produced as a result of the structure of MWCnT. At a flow velocity of 2.5 liters per minute and a concentration of 0.15 percent nanoparticles, the HTC is highest for both types of nanofluids. At a nanoparticle concentration of 0.15 percent and a flow rate of 2.5 liters per minute, the HTC of GnP nanofluid is higher than that of MWCnT nanofluid. It is possible to draw the conclusion that Graphene nanoparticles offer superior performance as a result.

From this numerical study the conclusion can be drawn that GnP nanofluids have better performance than MWCnT nanofluids.

References

[1] W. Yu, H. Xie, L. Chen, and Y. Li, "Enhancement of thermal conductivity of kerosene-based Fe3O4 nanofluids prepared via phase-transfer method," *Colloids Surfaces A Physicochem. Eng. Asp.*, vol. 355, no. 1–3, pp. 109–113, 2010, doi: 10.1016/j.colsurfa.2009.11.044.

[2] K. Wusiman, H. Jeong, K. Tulugan, H. Afrianto, and H. Chung, "Thermal performance of multi-walled carbon nanotubes (MWCNTs) in aqueous suspensions with surfactants SDBS and SDS," *Int. Commun. Heat Mass Transf.*, vol. 41, pp. 28–33, 2013, doi: 10.1016/j.icheatmasstransfer.2012.12.002.

[3] Y. Li, J. Zhou, S. Tung, E. Schneider, and S. Xi, "A review on development of nanofluid preparation and characterization," *Powder Technol.*, vol. 196, no. 2, pp. 89–101, 2009, doi: 10.1016/j.powtec.2009.07.025.

[4] W. Yu, H. Xie, and W. Chen, "Experimental investigation on thermal conductivity of nanofluids containing graphene oxide nanosheets," *J. Appl. Phys.*, vol. 107, no. 9, 2010, doi: 10.1063/1.3372733.

[5] A. Naddaf and S. Zeinali Heris, "Experimental study on thermal conductivity and electrical conductivity of diesel oil-based nanofluids of graphene nanoplatelets and carbon nanotubes," *Int. Commun. Heat Mass Transf.*, vol. 95, pp. 116–122, 2018, doi: 10.1016/j.icheatmasstransfer.2018.05.004.

[6] E. Sadeghinezhad *et al.*, "A comprehensive review on graphene nanofluids: Recent research, development and applications," *Energy Convers. Manag.*, vol. 111, pp. 466–487, 2016, doi: 10.1016/j.enconman.2016.01.004.

[7] M. M. Sarafraz, B. Yang, O. Pourmehran, M. Arjomandi, and R. Ghomashchi, "Fluid and heat transfer characteristics of aqueous graphene nanoplatelet (GNP) nanofluid in a microchannel," *Int. Commun. Heat Mass Transf.*, vol. 107, pp. 24–33, 2019, doi: 10.1016/j.icheatmasstransfer.2019.05.004.

[8] U. Calviño, J. P. Vallejo, M. H. Buschmann, J. Fernández-seara, and L. Lugo, "Analysis of heat transfer characteristics of a GnP aqueous nanofluid through a double-tube heat exchanger," *Nanomaterials*, vol. 11, no. 4, 2021, doi: 10.3390/nano11040844.

[9] O. Almatar AbdRabbuh *et al.*, "An experimental investigation of eco-friendly treated GNP heat transfer growth: circular and square conduit comparison," *J. Therm. Anal. Calorim.*, vol. 145, no. 1, pp. 139–151, 2021, doi: 10.1007/s10973-020-09652-5.

[10] M. Mehrali *et al.*, "Effect of specific surface area on convective heat transfer of graphene nanoplatelet aqueous nanofluids," *Exp. Therm. Fluid Sci.*, vol. 68, pp. 100–108, 2015, doi: 10.1016/j.expthermflusci.2015.03.012.

[11] A. Ghozatloo, A. Rashidi, and M. Shariaty-Niassar, "Convective heat transfer enhancement of graphene nanofluids in shell and tube heat exchanger," *Exp. Therm. Fluid Sci.*, vol. 53, pp. 136–141, 2014, doi: 10.1016/j.expthermflusci.2013.11.018.

[12] M. Naraki, S. M. Peyghambarzadeh, S. H. Hashemabadi, and Y. Vermahmoudi, “Parametric study of overall HTC of CuO/water nanofluids in a car radiator,” *Int. J. Therm. Sci.*, vol. 66, pp. 82–90, 2013, doi: 10.1016/j.ijthermalsci.2012.11.013.

[13] A. M. Hussein, K. V. Sharma, R. A. Bakar, and K. Kadirgama, “Heat Transfer Enhancement with Nanofluids – A Review,” *J. Mech. Eng. Sci.*, vol. 4, no. June, pp. 452–461, 2013, doi: 10.15282/jmes.4.2013.9.0042.

[14] G. Huminic and A. Huminic, “Heat transfer characteristics in double tube helical heat exchangers using nanofluids,” *Int. J. Heat Mass Transf.*, vol. 54, no. 19–20, pp. 4280–4287, 2011, doi: 10.1016/j.ijheatmasstransfer.2011.05.017.

[15] X. Yimin and L. Qiang, “SCIENCE IN CHINA (Series E) Convective heat transfer and flow characteristics of Cu-water nanofluid,” *Convect. heat Transf.*, vol. 45, no. 4, 2002.

[16] W. Duangthongsuk and S. Wongwises, “Heat transfer enhancement and pressure drop characteristics of TiO2-water nanofluid in a double-tube counter flow heat exchanger,” *Int. J. Heat Mass Transf.*, vol. 52, no. 7–8, pp. 2059–2067, 2009, doi: 10.1016/j.ijheatmasstransfer.2008.10.023.

[17] C. T. Nguyen, G. Roy, C. Gauthier, and N. Galanis, “Heat transfer enhancement using Al2O3-water nanofluid for an electronic liquid cooling system,” *Appl. Therm. Eng.*, vol. 27, no. 8–9, pp. 1501–1506, 2007, doi: 10.1016/j.applthermaleng.2006.09.028.

[18] M. Zarringhalam, A. Karimipour, and D. Toghraie, “Experimental study of the effect of solid volume fraction and Reynolds number on HTC and pressure drop of CuO-Water nanofluid,” *Exp. Therm. Fluid Sci.*, vol. 76, pp. 342–351, 2016, doi: 10.1016/j.expthermflusci.2016.03.026.

[19] S. Baskar, M. Chandrasekaran, T. Vinod Kumar, P. Vivek, and L. Karikalan, “Experimental studies on convective HTC of water/ethylene glycol-carbon nanotube nanofluids,” *Int. J. Ambient Energy*, vol. 41, no. 3, pp. 296–299, 2020, doi: 10.1080/01430750.2018.1451381.

[20] B. Farajollahi, S. G. Etemad, and M. Hojjat, “Heat transfer of nanofluids in a shell and tube heat exchanger,” *Int. J. Heat Mass Transf.*, vol. 53, no. 1–3, pp. 12–17, 2010, doi: 10.1016/j.ijheatmasstransfer.2009.10.019.

[21] M. R. Safaei, H. Togun, K. Vafai, S. N. Kazi, and A. Badarudin, “Investigation of heat transfer enhancement in a forward-facing contracting channel using FMWCNT nanofluids,” *Numer. Heat Transf. Part A Appl.*, vol. 66, no. 12, pp. 1321–1340, 2014, doi: 10.1080/10407782.2014.916101.

[22] A. V. Minakov, D. V. Guzei, M. I. Pryazhnikov, V. A. Zhigarev, and V. Y. Rudyak, “Study of turbulent heat transfer of the nanofluids in a cylindrical channel,” *Int. J. Heat Mass Transf.*, vol. 102, pp. 745–755, 2016, doi: 10.1016/j.ijheatmasstransfer.2016.06.071.

[23] S. Kim *et al.*, “Experimental investigation of HTC with Al2O3 nanofluid in small diameter tubes,” *Appl. Therm. Eng.*, vol. 146, pp. 346–355, 2019, doi: 10.1016/j.applthermaleng.2018.10.001.

[24] F. Rashidi and N. M. Nezamabad, “Experimental investigation of convective HTC of CNTs nanofluid under constant heat flux,” *Proc. World Congr. Eng. 2011, WCE 2011*, vol. 3, pp. 2441–2446, 2011.

[25] K. B. Anoop, T. Sundararajan, and S. K. Das, “Effect of particle size on the convective heat transfer in nanofluid in the developing region,” *Int. J. Heat Mass Transf.*, vol. 52, no. 9–10, pp. 2189–2195, 2009, doi: 10.1016/j.ijheatmasstransfer.2007.11.063.

[26] E. Ebrahimnia-Bajestan, H. Niazmand, W. Duangthongsuk, and S. Wongwises, “Numerical investigation of effective parameters in convective heat transfer of nanofluids flowing under a laminar flow regime,” *Int. J. Heat Mass Transf.*, vol. 54, no. 19–20, pp. 4376–4388, 2011, doi: 10.1016/j.ijheatmasstransfer.2011.05.006.

[27] Y. Gao, H. Wang, A. P. Sasmito, and A. S. Mujumdar, “Measurement and modeling of thermal conductivity of graphene nanoplatelet water and ethylene glycol base nanofluids,” *Int. J. Heat Mass Transf.*, vol. 123, pp. 97–109, 2018, doi: 10.1016/j.ijheatmasstransfer.2018.02.089.

[28] M. Corcione, “Empirical correlating equations for predicting the effective thermal conductivity and dynamic viscosity of nanofluids,” *Energy Convers. Manag.*, vol. 52, no. 1, pp. 789–793, 2011, doi: 10.1016/j.enconman.2010.06.072.

[29] S. E. B. Maïga, C. T. Nguyen, N. Galanis, and G. Roy, “Heat transfer behaviours of nanofluids in a uniformly heated tube,” *Superlattices Microstruct.*, vol. 35, no. 3–6, pp. 543–557, 2004, doi: 10.1016/j.spmi.2003.09.012.

[30] V. Bianco, O. Manca, and S. Nardini, “Second law analysis of A L 2 O 3 - water nanofluid turbulent forced convection in a circular cross section tube with constant wall Temperature,” *Adv. Mech. Eng.*, vol. 2013, 2013, doi: 10.1155/2013/920278.

[31] M. Edalatpour and J. P. Solano, “Thermal-hydraulic characteristics and exergy performance in tube-on-sheet flat plate solar collectors: Effects of nanofluids and mixed convection,” *Int. J. Therm. Sci.*, vol. 118, pp. 397–409, 2017, doi: 10.1016/j.ijthermalsci.2017.05.004.

[32] H. Masuda, A. Ebata, K. Teramae, and N. Hishinuma, “Alteration of Thermal Conductivity and Viscosity of Liquid by Dispersing Ultra-Fine Particles. Dispersion of Al2O3, SiO2 and TiO2 Ultra-Fine Particles.,” *Netsu Bussei*, vol. 7, no. 4, pp. 227–233, 1993, doi: 10.2963/jjtp.7.227.

[33] H. E. Patel, T. Sundararajan, and S. K. Das, “An experimental investigation into the thermal conductivity enhancement in oxide and metallic nanofluids,” *J. Nanoparticle Res.*, vol. 12, no. 3, pp. 1015–1031, 2010, doi: 10.1007/s11051-009-9658-2.